

# Time-dependent Hamiltonian Simulation via Magnus Expansion: Algorithm and Superconvergence

Di Fang<sup>1,2</sup>, Diyi Liu<sup>3</sup>, and Rahul Sarkar<sup>4</sup>

<sup>1</sup>*Department of Mathematics, Duke University*

<sup>2</sup>*Duke Quantum Center, Duke University*

<sup>3</sup>*School of Mathematics, University of Minnesota-Twin Cities*

<sup>4</sup>*Institute for Computational and Mathematical Engineering, Stanford University*

## Abstract

Hamiltonian simulation becomes more challenging as the underlying unitary becomes more oscillatory. In such cases, an algorithm with commutator scaling and a weak dependence, such as logarithmic, on the derivatives of the Hamiltonian is desired. We introduce a new time-dependent Hamiltonian simulation algorithm based on the Magnus expansion that exhibits both features. Importantly, when applied to unbounded Hamiltonian simulation in the interaction picture, we prove that the commutator in the second-order algorithm leads to a surprising fourth-order superconvergence, with an error preconstant independent of the number of spatial grids. This extends the qHOP algorithm [An, Fang, Lin, Quantum 2022] based on first-order Magnus expansion, and the proof of superconvergence is based on semiclassical analysis that is of independent interest.

## Contents

<b>1</b>	<b>Introduction</b>	<b>2</b>
<b>2</b>	<b>Magnus expansion and algorithm overview</b>	<b>4</b>
<b>3</b>	<b>Error representation</b>	<b>6</b>
3.1	Truncation error of the Magnus series . . . . .	6
3.2	Quadrature errors of the Magnus series . . . . .	10
3.3	Long-time algorithm error . . . . .	11
<b>4</b>	<b>Superconvergence</b>	<b>11</b>
4.1	Heuristic intuition . . . . .	11
4.2	Rigorous proof of superconvergence . . . . .	12
<b>5</b>	<b>Circuit construction</b>	<b>14</b>
5.1	Input model . . . . .	15
5.1.1	Input model for $H(t)$ . . . . .	15
5.1.2	Input model for interaction picture . . . . .	15

5.2	Quantum circuit for second-order Magnus expansion . . . . .	15
5.3	Long-time complexity of second-order Magnus expansion . . . . .	18
<b>6</b>	<b>Conclusion and discussion</b>	<b>21</b>
<b>A</b>	<b>Proof of the key commutator estimate</b>	<b>22</b>
<b>B</b>	<b>Proof of Lemma 7</b>	<b>25</b>

# 1 Introduction

Simulation of quantum dynamics, emerging as the original motivation for quantum computers [1], is widely viewed as one of the most important applications of a quantum computer. Quantum algorithms for Hamiltonian simulations aim to construct good approximations of the unitary evolution operator. When the Hamiltonian varies slowly with respect to time or when polynomial dependence on the time derivatives of the Hamiltonian is acceptable, many numerical integrators can yield satisfactory performance, including the standard Trotterization and classical Magnus integrators. However, major challenges arise when the unitary exhibits highly oscillatory behavior, typically caused by the large operator norm of the Hamiltonian and rapid changes of the Hamiltonian itself in a time-dependent scenario. A wide range of applications fall into one or both categories including, e.g., adiabatic quantum computation [2, 3],  $k$ -local Hamiltonians (with a large number of sites) [4–7], the electronic structure problem and molecular dynamics (with a real space discretization) [8–14], bosonic systems [15, 16], quantum control problems with ultrafast lasers [17–19], interaction picture Hamiltonian simulation [20, 21], and quantum-based optimization solvers [22–24].

Recent advancements in quantum algorithms have notably improved error bounds for managing oscillatory dynamics. For time-independent Hamiltonians, Trotter-type algorithms leverage commutator scaling to achieve asymptotic improvements in many applications (pioneered by [6, 25] and other specific case based analysis such as [11, 13, 26–33]). Recent developments have revealed that multiproduct formulas also exhibit commutator scaling [34–36]. Conversely, the benefits of commutator scaling for time-dependent Hamiltonians are less understood. The generalized Trotter formulas [11, 37] and multiproduct based on discrete-clock construction [34] can display commutator scaling when the time-dependent Hamiltonian is in a controlled form, namely,  $H(t) = \sum_j c_j(t)U_j$  with  $c_j$  being scalar functions so that the time-order evolution governed by each of the components become not time-ordered. Nevertheless, efficiently handling time-ordered unitaries for general cases remains a challenge, and further approximation to such time-ordered operators can compromise the commutator scaling [11] and introduce polynomial overhead on the time-derivatives of the Hamiltonian [38] for standard Trotter formulas. On the other hand, both truncated Dyson series based method [20, 39–41] and randomized based methods [21, 41, 42] can obtain complexity scaling insensitive to the fast change of the Hamiltonian. Such algorithms, however, depend on the operator norm of the Hamiltonian instead of the commutator.

For general time-dependent Hamiltonian simulation, a quantum algorithm that features both commutator scaling and logarithmic dependence on the derivatives was first proposed in [43]. It considers the exploration of directly implementing the Magnus series truncation as a quantum algorithm. Unlike the standard Trotter formulas or classical geometric integrators, this method implements a highly accurate numerical quadrature with many quadrature points as many as the norm of the derivative,  $\|H'(t)\|$ , to reduce the quadrature error to the same level as the truncation

error induced by truncating the Magnus series. This quadrature rule can be efficiently implemented via the linear combination of unitaries (LCU) technique with only a logarithmic cost overhead dependent on the number of quadrature points and hence the norm of the derivative of  $H$ . Essentially, the qHOP algorithm introduced in [43] functions as a non-interpolatory Magnus integrator, and it truncates the Magnus series to the first order. It is also shown that first-order Magnus expansion in the interaction picture paired with one quadrature point gives rise to the first and second-order Trotter formulas. Another significant line of development on quantum algorithms based on Magnus series [44–46] further combines the Magnus series with product formulas, in which case the number of quadrature points will enter polynomially into the number of products in the Trotterization procedure. Such methodologies are efficient for a number of physically motivated applications, including geometrically local Hamiltonians across all three cited works. In particular, [44] considers those under a small geometrically local perturbation, and the framework leverages quasi-locality and can lead to optimal scaling for various regimes. In this work, we follow the LCU-line, and develop a quantum circuit to implement the second-order Magnus truncation.

Another relevant line is classical algorithms based on the Magnus series. Classically, the Magnus expansion is used to design Magnus integrators, which have been extensively studied and widely used in literature (see, e.g., [47–57]). The idea is to first approximate the time-ordered exponential with a regular exponential using the Magnus series expansion, followed by the application of suitable quadrature rules featuring a few quadrature points, such as Gauss-Legendre quadrature. This inevitably introduces a polynomial overhead on the derivatives of the Hamiltonian for general cases. The implementation of this framework as a quantum algorithm has been recently developed in [58] for time-dependent spin systems in the controlled form, in which case the commutators in Magnus expansion can be calculated explicitly by hand.

### Contribution:

In this work, we develop a quantum algorithm for general time-dependent Hamiltonian simulation based on the second-order Magnus series truncation and prove that the algorithm not only achieves commutator scaling in the high precision regime but also exhibits a logarithmic dependency on the derivatives of the Hamiltonian  $H(t)$ . We show that for general time-dependent Hamiltonians, the algorithm is of second order with a commutator scaling and logarithmic dependence on the derivative in the cost. When allowing polynomial derivative dependence in the cost, the algorithm can achieve up to fourth-order convergence. As a direct application, our algorithm provides an efficient way of simulating Hamiltonian in the interaction picture and hence can be useful in the time-independent Hamiltonian simulation as well. Moreover, we prove that our method achieves **superconvergence** for the digital simulation of the Schrödinger equation (also called unbounded Hamiltonian simulation or real-space Hamiltonian simulation in the literature). Surprisingly, the second order Magnus series truncation can achieve a *fourth* order superconvergence for the Schrödinger equation in the interaction picture and importantly with an error preconstant *independent* of  $A$  (or the number of degrees of freedom  $N$  used to discretize the differential operator). This can be crucial for improved efficiency for unbounded Hamiltonian, as the number of degrees of freedom in the spatial discretization can be huge. Note that this is completely different from a fourth-order convergence with a preconstant polynomially dependent on the derivatives of  $H(t)$ , as for the interaction pictured Hamiltonian  $H(t) = e^{iAt} B e^{-iAt}$ , where  $A$  and  $B$  are the spatial discretizations of the Laplacian and potential respectively, its derivative is dependent on  $A$  and hence the number of grid points in a polynomial fashion.

We remark that the superconvergence result is one of its own kind that goes beyond the typical

order improvement behavior for many algorithms due to the cancellation of high-order terms in the Taylor expansion. For unbounded Hamiltonian simulation, as will be detailed in Section 4.1, performing Taylor expansion to the numerical approximation in fact can not lead to the superconvergence result due to the introduction of the derivative dependence in the Taylor expansion procedure. A superconvergence result for the first-order Magnus series expansion has been proved in [43], which shows that the first-order Magnus series expansion exhibits second-order superconvergence. It has also been conjectured that the Magnus series expansion with second-order truncation exhibits fourth-order superconvergence, while the proving machinery proposed there can only establish a third-order convergence. In this work, we prove the fourth-order superconvergence rigorously. Notably, if one tries to do this naively, one runs into severe problems due to an explosion of the number of terms for which one needs to prove commutator estimates. In fact, this does not work, as many terms were unbounded operators on  $L^2$  (see Section 4.1 for details). The way we managed to make some headway into this proof is to utilize tools from semiclassical microlocal analysis. A key commutator estimate with unbounded operators has been established using the semiclassical pseudodifferential operator machinery. As a byproduct, we also rederive the second-order superconvergence result of the first-order Magnus expansion proved in [43] using the semiclassical machinery in an elegant manner.

**Organization:**

The rest of this paper is organized as follows. In Section 2 we discuss the Magnus series and the second-order Magnus expansion. We then introduce a quantum algorithm based on the second-order Magnus series expansion. Section 3 focuses on the error analysis for the general time-dependent Hamiltonian, including both the Magnus truncation error and the numerical quadrature error. We then establish the superconvergence in Section 4 by first providing a heuristic intuition which also explains why the usual Taylor expansion route can not work, and then providing a rigorous proof of the superconvergence based on semiclassical analysis. Section 5 discusses the circuit construction of the algorithm for both general time-dependent Hamiltonians and in the interaction picture. Finally, in Section 6, we conclude with some further remarks.

## 2 Magnus expansion and algorithm overview

We consider the time-dependent Hamiltonian simulation problem, which involves computing the solution to

$$i\partial_t u(t) = H(t)u(t), \quad u(t) = u_0. \tag{1}$$

Throughout the work, we mainly explore two cases: one for general  $H(t)$ , and the other for the time-dependent Hamiltonian in the interaction picture. Note that the latter is an equivalent formulation of a (potentially time-independent) Hamiltonian simulation where the Hamiltonian  $H = A + B(t)$ , with  $\|A\| \gg \|B\|$ . Throughout the paper, we use  $\|\cdot\|$  to denote the spectral norm for finite-dimensional operators, which can be infinite for unbounded operators. Here  $A$  and  $B(t)$  are both Hermitian and  $A$  is fast-forwardable, which means its time evolution can be efficiently implemented sublinear in time such as a diagonal matrix [59]. Later, we make explicit the oracle input in Section 5.1. In this scenario, the interaction-picture Hamiltonian [20] becomes  $H_I(t) = e^{iAt}B(t)e^{-iAt}$ , so that the original Hamiltonian simulation problem can be equivalently solved by

$$e^{-itH} = e^{-it(A+B)} = e^{-iAt} \mathcal{T} e^{-i \int_0^t H_I(s) ds}. \tag{2}$$

We now discuss the Magnus expansion and construction of our algorithm. For simplicity, we denote  $A(t) := -iH(t)$ . The exact solution of the equation

$$\dot{u}(t) = A(t)u(t), \quad u(0) = u_0, \quad (3)$$

can be expressed as

$$u(t) = \mathcal{T} \left( \exp \int_0^t A(s) ds \right) u_0. \quad (4)$$

We note that, on a rigorous level, the time-ordered exponential is defined by a series expansion, which may not always be well-defined as a convergent series, especially for unbounded operators. Throughout this work, we use the time-ordered exponential as a formal notation to represent the underlying unitary operator that is well-defined. In contrast, the Magnus series provides an alternative expression of the propagator without the time-ordering operator

$$u(t) = \exp(\Omega(t))u_0, \quad (5)$$

where

$$\frac{d\Omega}{dt} = \sum_{n=0}^{\infty} \frac{B_n}{n!} \text{ad}_{\Omega}^n A. \quad (6)$$

Here  $B_n$  are the Bernoulli numbers with  $B_1 = -1/2$ , and the ad operator follows the standard definition  $\text{ad}_{\Omega}(C) = [\Omega, C]$  and  $\text{ad}_{\Omega}^{k+1}(C) = [\Omega, \text{ad}_{\Omega}^k(C)]$ . Equivalently, we have the infinite series for  $\Omega$  given as

$$\Omega(t) = \sum_{n=1}^{\infty} \Omega^{(n)}(t), \quad (7)$$

$$\Omega^{(n)}(t) = \sum_{j=1}^{n-1} \frac{B_j}{j!} \sum_{\substack{k_1 + \dots + k_j = n-1 \\ k_1 \geq 1, \dots, k_j \geq 1}} \int_0^t \text{ad}_{\Omega^{(k_1)}(s)} \text{ad}_{\Omega^{(k_2)}(s)} \cdots \text{ad}_{\Omega^{(k_j)}(s)} A(s) ds \quad n \geq 2. \quad (8)$$

The first few terms of  $\Omega$  are

$$\Omega(t) = \int_0^t A(t_1) dt_1 - \frac{1}{2} \int_0^t \left[ \int_0^{t_1} A(t_2) dt_2, A(t_1) \right] dt_1 + \cdots. \quad (9)$$

More detailed discussion on Magnus series can be found in, e.g., the review [53].

In this work, we consider the second-order Magnus series truncation, namely, the propagator is approximated as

$$\mathcal{T} \left( \exp \int_0^t A(s) ds \right) \approx e^{\Omega_2(t)}, \quad \Omega_2(t) := \int_0^t A(s) ds - \frac{1}{2} \int_0^t \left[ \int_0^s A(\sigma) d\sigma, A(s) \right] ds. \quad (10)$$

In this case, we also have

$$\dot{\Omega}_2(t) := A(t) - \frac{1}{2} \left[ \int_0^t A(\sigma) d\sigma, A(t) \right]. \quad (11)$$

To discretize and approximate the exact evolution operator, we first divide the entire time interval  $[0, T]$  into  $L$  equally spaced segments. Let the time step size  $h = T/L$  and  $t_j = jh$ , then

$$U_{\text{exact}}(T, 0) = \prod_{j=0}^{L-1} U_{\text{exact}}(t_j + h, t_j) = \prod_{j=0}^{L-1} \mathcal{T} e^{-i \int_{t_j}^{t_j+h} H(s) ds}. \quad (12)$$

We then utilize the second-order Magnus series expansion to approximate each sub-interval, namely,

$$U_{\text{exact}}(t_j + h, t_j) \approx e^{\Omega_2(t_j+h, t_j)} := U_2(t_j + h, t_j), \quad (13)$$

where

$$\Omega_2(t_j + h, t_j) := \int_{t_j}^{t_j+h} A(s) ds - \frac{1}{2} \int_{t_j}^{t_j+h} \left[ \int_{t_j}^s A(\sigma) d\sigma, A(s) \right] ds. \quad (14)$$

The numerical quadratures are then conducted with an exceedingly precise quadrature using  $M$  quadrature points, where  $M$  denotes a large number.

$$\Omega_2(t_j+h, t_j) \approx -i \sum_{p=0}^{M-1} H\left(t_j + \frac{ph}{M}\right) \frac{h}{M} + \frac{1}{2} \sum_{p=0}^{M-1} \left[ \sum_{q=1}^p H\left(t_j + \frac{qh}{M}\right) \frac{h}{M}, H\left(t_j + \frac{ph}{M}\right) \right] \frac{h}{M} := \tilde{\Omega}_2(t_j+h, t_j). \quad (15)$$

As to be detailed in Section 3.2, we devise an LCU-type quantum circuit to enact  $\tilde{\Omega}_2(t_j + h, t_j)$  and subsequently apply the quantum singular value transformation (QSVT) combined with oblivious amplitude amplification (OAA) to compute the matrix exponential  $\exp\left(\tilde{\Omega}_2(t_j + h, t_j)\right)$  and the long-time evolution is the product

$$\tilde{U}_2(t_j + h, t_j) := \exp\left(\tilde{\Omega}_2(t_j + h, t_j)\right), \quad \tilde{U}_2(T, 0) = \prod_{j=0}^{L-1} \tilde{U}_2(t_j + h, t_j). \quad (16)$$

### 3 Error representation

In this section, we present the error analysis for our algorithm for general  $H(t)$ . There are two sources of errors: the truncation error of the Magnus series and the numerical quadrature error. For the truncation error, we prove two bounds – one with a commutator scaling, and another higher order estimate if allowing for the derivative dependence of the Hamiltonian  $H(t)$ . We then discuss the quadrature error with  $M$  quadrature points. Finally, we sum both errors and present the algorithm error estimate over the long time  $[0, T]$ .

#### 3.1 Truncation error of the Magnus series

In order to obtain the error representation between the exact propagator  $U_{\text{exact}}(t_j + h, t_j) := \mathcal{T}\left(\exp \int_{t_j}^{t_j+h} A(s) ds\right)$  and the second-order Magnus truncation  $U_2(t_j + h, t_j) := e^{\Omega_2(t_j+h, t_j)}$ , we follow the usual way in numerical analysis to consider their corresponding differential equations and utilize the variation of constants formula. In particular, suppose  $U_2$  satisfying

$$\dot{U}_2 = \tilde{A}U_2, \quad (17)$$

then the error between  $U_{\text{exact}}$  and  $U_2$  can be estimated as

$$\|U_{\text{exact}} - U_2\| = \int_{t_j}^{t_j+h} \|\tilde{A}(s) - A(s)\| ds, \quad (18)$$

where we use the variation of constant formula and the fact that the underlying dynamics are unitary.

For notational simplicity, we describe the proof idea for the difference between  $U_{\text{exact}}(t) := U_{\text{exact}}(t, 0)$  and  $U_2(t) := U_2(t, 0)$  over a short time interval  $[0, t]$ . The same procedure applies to general intervals  $[t_j, t_j + h]$ , as detailed in the proof of Theorem 1. We now try to make explicit the expression of  $\tilde{A}$ . By [53, Lemma 2], the derivative of  $U_2$  is

$$\dot{U}_2 = \frac{d}{dt} \exp(\Omega_2(t)) = d \exp_{\Omega_2(t)}(\dot{\Omega}_2(t)) \exp(\Omega_2(t)) = d \exp_{\Omega_2(t)}(\dot{\Omega}_2(t)) U_2, \quad (19)$$

where

$$d \exp_{\Omega}(C) = \sum_{k=0}^{\infty} \frac{1}{(k+1)!} \text{ad}_{\Omega}^k(C) = \frac{\exp(\text{ad}_{\Omega}) - I}{\text{ad}_{\Omega}}(C) \quad (20)$$

and the ad operator follows the usual definition  $\text{ad}_{\Omega}(C) = [\Omega, C]$  and  $\text{ad}_{\Omega}^{k+1}(C) = [\Omega, \text{ad}_{\Omega}^k(C)]$ . Therefore, we obtain the expression of  $\tilde{A}$  as

$$\tilde{A}(t) = d \exp_{\Omega_2(t)}(\dot{\Omega}_2) = \dot{\Omega}_2 + \frac{1}{2}[\Omega_2, \dot{\Omega}_2] + \frac{1}{6}[\Omega_2, [\Omega_2, \dot{\Omega}_2]] + g(\text{ad}_{\Omega_2})(\text{ad}_{\Omega_2}^3(\dot{\Omega}_2)), \quad (21)$$

where  $r_4$  is the remainder term in the series expansion of the function  $\frac{e^z - 1}{z}$

$$\frac{e^z - 1}{z} = 1 + \frac{1}{2}z + \frac{1}{6}z^2 + g(z)z^3, \quad (22)$$

or  $g(z) = \frac{1}{2\pi i} \int_{\gamma} \frac{e^w - 1}{w^4(w-z)} dw$ , where  $\gamma$  is a simple closed positive oriented contour with  $z$  being an interior point. Here, we only need to expand to this order because  $\Omega_2$  involves integrals of one layer and two layers, while  $\dot{\Omega}_2$  involves a term without an integral. Therefore,  $\text{ad}_{\Omega_2}^3(\dot{\Omega}_2)$  already contains at least 3 layers of time integrals (contributing to  $t^3$ ). If the nested commutators can contribute at least another power of  $t$ , along with  $g$ , this remainder term is expected to be upper-bounded by  $t^4$ . We will show in this section that this is true if one allows derivative dependence in the error bound for general  $H(t)$ . Furthermore, if we are in the case of superconvergence, the error preconstant does not depend on the derivative of  $A(t)$  (to be proved in Section 4.2).

Substituting Eq. (10) and Eq. (11) to (21), we have

$$\begin{aligned} \tilde{A}(t) - A(t) &= -\frac{1}{2} \left[ \int_0^t A(\sigma) d\sigma, A(t) \right] \\ &+ \frac{1}{2} \left[ \int_0^t A(s) ds - \frac{1}{2} \int_0^t \left[ \int_0^s A(\sigma) d\sigma, A(s) \right] ds, A(t) - \frac{1}{2} \left[ \int_0^t A(\sigma) d\sigma, A(t) \right] \right] \\ &+ \frac{1}{6} \left[ \int_0^t A(s) ds - \frac{1}{2} \int_0^t \left[ \int_0^s A(\sigma) d\sigma, A(s) \right] ds, \left[ \int_0^t A(s) ds - \frac{1}{2} \int_0^t \left[ \int_0^s A(\sigma) d\sigma, A(s) \right] ds, A(t) - \frac{1}{2} \left[ \int_0^t A(\sigma) d\sigma, A(t) \right] \right] \right] \\ &+ g(\text{ad}_{\Omega_2})(\text{ad}_{\Omega_2}^3(\dot{\Omega}_2)) \end{aligned}$$

Note that terms with a single layer of integral vanish, while terms with double-layered integrals can be expressed as:

$$\left[ \int_0^t A(s) ds, \left[ \int_0^t A(s) ds, A(t) \right] \right] + 3 \int_0^t ds \int_0^s d\sigma [[A(\sigma), A(s)], A(t)] := I_1 \quad (23)$$

The remaining terms include  $g(\text{ad}_{\Omega_2})(\text{ad}_{\Omega_2}^3(\dot{\Omega}_2)) := I_2$  and eight terms denoted as  $I_3$ , each characterized by a minimum of three layers of time integrals and a minimum of three layers of nested commutators with respect to  $A$ . Note that all terms admit a nested commutator format.

In order to show superconvergence for the real-space Hamiltonian in the first quantization, it suffices to show that  $I_1$ ,  $I_2$ , and  $I_3$  all exhibit  $\mathcal{O}(t^4)$  behavior, where the error preconstant depends solely on  $B = V(x)$ . We note that the more layers the integrals and commutators are, the easier the terms can be controlled, as each layer of the time integral essentially contributes to one more order in  $t$ . Therefore, the crucial estimate to establish is to estimate  $I_1$  as defined in Eq. (23). We will prove the superconvergence in Section 4.2.

We now turn our attention to the general time-dependent  $H(t)$ . We will demonstrate that if we seek a bound independent of the derivative of  $H(t)$ , we can bound  $\|\tilde{A} - A(t)\|$  with  $\mathcal{O}(t^2)$ . If we permit the derivative of  $H$  to influence the preconstant, the bound can be improved to  $\mathcal{O}(t^4)$ . However, it is important to note that this latter case does not represent superconvergence, since in the interaction picture, the derivative of  $H_I(t) = e^{iAt} B e^{-iAt}$  still depends on  $A$ . We also note that while we currently bound nested commutators of more than three layers using the three-layer ones, a tighter bound could be achieved by making explicit the contributions of the higher orders of nested commutators.

**Theorem 1** (Local truncation error for general  $H(t)$ ). *Consider the exact propagator  $U_{\text{exact}}(t, s) = \mathcal{T} \exp\left(-i \int_s^t H(s) ds\right)$  and the second-order Magnus truncation  $U_2(t, s) := e^{\Omega_2(t, s)}$ , where  $\Omega_2(t, s)$  is defined as Eq. (14). If the Hamiltonian satisfies  $\|H(t)\| \leq \alpha$  and the nested commutator satisfies*

$$\sup_{s, t, \tau \in [t_j, t_{j+1}]} \|[H(\tau), [H(s), H(t)]]\| \leq C_{\text{comm}},$$

then for any  $h \leq c/\alpha$  with some absolute constant  $c$ , we have

$$\|U_{\text{exact}}(t_{j+1}, t_j) - U_2(t_{j+1}, t_j)\| \leq C \min\{C_{\text{comm}} h^3, C'_H h^5\}, \quad (24)$$

where  $C$  is some absolute constant and  $C'_H$  is some prefactor that depends on  $\alpha$ , as well as the norms of the derivatives  $\sup_{t \in [t_j, t_{j+1}]} \left\| \frac{d^p}{dt^p} H(t) \right\|$  for  $p = 1, 2$ .

*Proof.* It suffices to bound the terms of  $I_1$ ,  $I_2$  and  $I_3$ , for which we will change the intervals of interest from  $[0, t]$  to  $[t_j, t_{j+1}]$ . For simplicity of notation, hereafter we will continue to denote these terms, even after changing the integral intervals, as  $I_1$ ,  $I_2$  and  $I_3$ .

We start by proving the first estimate of  $CC_{\text{comm}}h^3$ . It follows immediately that

$$\|I_1\| \leq CC_{\text{comm}}h^2, \quad (25)$$

with some absolute constant  $C$ . We now consider  $I_3$ , as mentioned before, all terms contain at least three layers of time integrals and a minimum of three layers of nested commutator with four  $A$  terms in one of the following forms

$$[[A(s), A(\tau)], [A(\sigma), A(t)]], \quad [A(s), [A(\tau), [A(\sigma), A(t)]]] \quad (26)$$

or additional nested commutator with them. The three layers of time integrals contribute to  $\mathcal{O}(h^3)$ , and the norms of the terms in Eq. (26) can all be upper bounded by

$$4 \sup_{t \in [t_j, t_{j+1}]} \|H(t)\| \sup_{s, t, \tau \in [t_j, t_{j+1}]} \|[H(\tau), [H(s), H(t)]]\|, \quad (27)$$

so that

$$\|I_3\| \leq Ch^3 C_{\text{comm}} \alpha \leq cCC_{\text{comm}}h^2, \quad (28)$$



where both  $c$  and  $C$  are some absolute constants. Finally, it follows from Lemma 7 as proved in Appendix B that

$$\|I_2\| \leq 2C \sup_{t \in [-h, h]} \|\Omega_2\| \left\| \text{ad}_{\Omega_2}^2(\dot{\Omega}_2) \right\|. \quad (29)$$

Note that  $\text{ad}_{\Omega_2}^2(\dot{\Omega}_2)$  is contained in the terms already estimated in  $I_1$  and  $I_3$  and hence has the norm bounded by  $CC'_{\text{comm}}h^2$ . Additionally,

$$\|\Omega_2\| \leq \alpha h + \alpha^2 h^2 \leq c + c^2. \quad (30)$$

This implies that

$$\|I_2\| \leq CC_{\text{comm}}h^2, \quad (31)$$

where  $C$  is again some absolute constant. We can conclude that

$$\|U_{\text{exact}}(t_{j+1}, t_j) - U_2(t_{j+1}, t_j)\| = \int_{t_j}^{t_j+h} \left\| \tilde{A}(s) - A(s) \right\| ds \leq CC_{\text{comm}}h^3. \quad (32)$$

We now proceed to prove the second estimate of  $CC'_Hh^5$ . Since derivatives are permissible within the bound, we can employ Taylor's theorem, which yields for  $t \in [t_j, t_{j+1}]$ ,

$$A(t) = A(t_j) + A'(t_j)(t - t_j) + \frac{1}{2}A''(\xi)(t - t_j)^2, \quad (33)$$

for some  $\xi \in [t_j, t_{j+1}]$ . One observation is that when plugging it into the nested commutator  $[A(s), [A(\tau), A(t)]]$ , there is no zeroth order term in terms of  $(t - t_j)$ . This implies that

$$\sup_{s, t, \tau \in [t_j, t_{j+1}]} \|[A(s), [A(\tau), A(t)]]\| = \sup_{s, t, \tau \in [t_j, t_{j+1}]} \|[H(\tau), [H(s), H(t)]]\| \leq C'_H h, \quad (34)$$

where  $C'_H$  depends on  $\alpha$  and the norms of the derivatives  $\left\| \frac{d^p}{dt^p} H(t) \right\|$  for  $p = 1, 2$ .

Consider substituting Eq. (33) into  $I_1$ . It is straightforward to check that the  $(t - t_j)^2$  terms in  $I_1$  are associated with  $[A(t_j), [A(t_j), A(t_j)]]$ , which is 0. Additionally, the  $(t - t_j)^3$  terms in  $I_1$  are associated with  $[A(t_j), [A(t_j), A'(t_j)]]$  and they cancel out exactly. The remaining terms are of order at least  $(t - t_j)^4$  and the prefactors depend on the nested commutators of elements from the set from  $\{A(t_j), A'(t_j), A''(\xi)\}$ . The norms of such nested commutators can be bounded by  $\alpha$  and the norms of the derivatives  $\left\| \frac{d^p}{dt^p} H(t) \right\|$  for  $p = 1, 2$ , so that we have

$$\|I_1\| \leq C'_H h^4. \quad (35)$$

For  $I_3$ , following a similar strategy as in the proof of the first estimate, we have

$$\|I_3\| \leq Ch^3 \sup_{t \in [t_j, t_{j+1}]} \|H(t)\| \sup_{s, t, \tau \in [t_j, t_{j+1}]} \|[H(\tau), [H(s), H(t)]]\| \quad (36)$$

$$\leq Ch^3 \alpha C'_H h = C\tilde{C}'_H h^4, \quad (37)$$

where  $\tilde{C}'_H$  depends on  $\alpha$  and  $\sup_{t \in [t_j, t_{j+1}]} \left\| \frac{d^p}{dt^p} H'(t) \right\|$ , for  $p = 1, 2$ . For  $I_2$ , applying Eq. (29), we have

$$\|I_2\| \leq C(\alpha h + \alpha^2 h^2)(C'_H + \tilde{C}'_H)h^4, \quad (38)$$

which can be further bounded by some  $C'_H$  times  $h^4$ . We can conclude that

$$\|U_{\text{exact}}(t_{j+1}, t_j) - U_2(t_{j+1}, t_j)\| = \int_{t_j}^{t_j+h} \left\| \tilde{A}(s) - A(s) \right\| ds \leq CC'_H h^5. \quad (39)$$

□

### 3.2 Quadrature errors of the Magnus series

We now discuss the quadrature error over the short time interval  $[t_j, t_j + h]$  for any  $j \in \{0, 1, \dots, L-1\}$ . We use a simple Riemann sum quadrature rule with  $M$  quadrature points. We choose this quadrature method because of its ease in constructing an LCU circuit, and it is also typically used in Dyson series implementations, e.g., [20, 43, 60, 61]. The approximation of the second-order Magnus truncation  $U_2(t_{j+1}, t_j)$  is denoted as  $\tilde{U}_2(t_{j+1}, t_j)$  and is defined as

$$\begin{aligned} \tilde{U}_2(t_{j+1}, t_j) &:= \exp(\tilde{\Omega}_2(t_j + h, t_j)) \\ &= \exp \left\{ -i \sum_{p=0}^{M-1} H(t_j + \frac{ph}{M}) \frac{h}{M} + \frac{1}{2} \sum_{p=0}^{M-1} \left[ \sum_{q=1}^p H(t_j + \frac{qh}{M}) \frac{h}{M}, H(t_j + \frac{ph}{M}) \right] \frac{h}{M} \right\}. \end{aligned} \quad (40)$$

We prove the quadrature error estimate for the general time-dependent Hamiltonian  $H(t)$ . We remark that it is possible to relax the bound of derivatives to bounded total variation (see [60]).

**Theorem 2** (Quadrature error for general  $H(t)$ ). *For  $U_2(t_{j+1}, t_j)$  defined as Eq. (13) and  $\tilde{U}_2(t_{j+1}, t_j)$  defined as Eq. (40), we have*

$$\left\| U_2(t_{j+1}, t_j) - \tilde{U}_2(t_{j+1}, t_j) \right\| \leq \frac{h^2}{M} \max_{s \in [t_j, t_{j+1}]} \|H'(s)\| + \frac{3h^3}{M} \max_{s \in [t_j, t_{j+1}]} \|H(s)\| \|H'(s)\|. \quad (42)$$

*Proof.* Note that for Hermitian matrices  $H_1$  and  $H_2$ , one has

$$\|e^{-iH_1 t} - e^{-iH_2 t}\| \leq \|t(H_1 - H_2)\|, \quad (43)$$

which follows from a direct application of the variation of the constant formula to the differential equations satisfied by the difference of the operators. Applying the inequality with  $t = 1$ , we can derive that

$$\begin{aligned} \left\| U_2(t_{j+1}, t_j) - \tilde{U}_2(t_{j+1}, t_j) \right\| &\leq \left\| \int_{t_j}^{t_{j+1}} H(s) ds - \sum_{p=0}^{M-1} H(t_j + \frac{ph}{M}) \frac{h}{M} \right\| \\ &+ \left\| \frac{1}{2} \int_{t_j}^{t_{j+1}} \left[ \int_{t_j}^s H(\sigma) d\sigma, H(s) \right] ds - \frac{1}{2} \sum_{p=0}^{M-1} \left[ \sum_{q=0}^{p-1} H(t_j + \frac{qh}{M}) \frac{h}{M}, H(t_j + \frac{ph}{M}) \right] \frac{h}{M} \right\|. \end{aligned} \quad (44)$$

By standard quadrature result [62], the first term of the right hand side can be bounded by

$$\frac{h^2}{M} \max_{s \in [t_j, t_{j+1}]} \|H'(s)\|. \quad (45)$$

The second term can be bounded as the summation of

$$\frac{h^2}{M} \max_{s \in [t_j, t_{j+1}]} \left\| \left[ \int_{t_j}^s H(\sigma) d\sigma, H'(s) \right] \right\| \leq \frac{2h^3}{M} \max_{s \in [t_j, t_{j+1}]} \|H(s)\| \|H'(s)\| \quad (46)$$

and

$$\frac{h^3}{M} \max_{s \in [t_j, t_{j+1}]} \|H(s)\| \|H'(s)\|. \quad (47)$$

□

For the interaction picture, the time-dependent Hamiltonian becomes  $H(t) = e^{iAt} B e^{-iAt}$ , where  $B$  can be potentially time-dependent, and the quadrature error estimate can be similarly derived. Here we present the case with time-independent  $B$ .

**Corollary 3** (Quadrature error for interaction picture). *For  $H(t) = e^{iAt} B e^{-iAt}$ ,  $U_2(t_{j+1}, t_j)$  defined as Eq. (13), and  $\tilde{U}_2(t_{j+1}, t_j)$  defined as Eq. (40), we have*

$$\left\| U_2(t_{j+1}, t_j) - \tilde{U}_2(t_{j+1}, t_j) \right\| \leq \frac{h^2}{M} \|[A, B]\| + \frac{3h^3}{M} \|B\| \|[A, B]\|. \quad (48)$$

*Proof.* The proof follows directly from Theorem 2.  $\square$

### 3.3 Long-time algorithm error

The sum of both errors in previous sections provides the short-time estimate. As all propagators are unitary, the error accumulates linearly in the number of time steps. We can summarize the algorithm error over the long time interval  $[0, T]$  as follows.

**Theorem 4** (long time error for general  $H(t)$ ). *Let  $U_{\text{exact}}(T, 0) = \mathcal{T} e^{-i \int_0^T H(s) ds}$  be the exact long-time propagator over the time interval  $[0, T]$ , and its numerical approximation  $\tilde{U}_2(T, 0)$  be*

$$\tilde{U}_2(t_L, t_{L-1}) \dots \tilde{U}_2(t_2, t_1) \tilde{U}_2(t_1, t_0). \quad (49)$$

*If the Hamiltonian satisfies  $\|H(t)\| \leq \alpha$ , then for  $h \leq c/\alpha$  for some constant  $c$ , the error satisfies*

$$\left\| U_{\text{exact}}(T, 0) - \tilde{U}_2(T, 0) \right\| \leq CT \left( \min \{ C_{\text{comm}} h^2, C'_H h^4 \} + \frac{h}{M} \max_{s \in [0, T]} \|H'(s)\| \right), \quad (50)$$

*where  $C$  is some absolute constant and  $C'_H$  is some prefactor that depends on  $\alpha$ , as well as the norms of the derivatives  $\sup_{t \in [0, T]} \left\| \frac{d^p}{dt^p} H(t) \right\|$  for  $p = 1, 2$ .*

*Proof.* The result follows directly from Theorem 1 and Theorem 2, together with the properties of unitary operators. Here the quadrature error is simplified to only one term due to the fact that  $h\alpha \leq c$ .  $\square$

## 4 Superconvergence

In this section, we delve into the superconvergence behavior in the case of  $A = \Delta$ , representing the Laplacian operator, and  $B = V(x)$ . First, we will explore heuristics that do *not* lead to superconvergence but are beneficial for understanding the intuition and challenges. Subsequently, we will present a rigorous proof of superconvergence, emphasizing the crucial estimates we are able to establish.

### 4.1 Heuristic intuition

We present a heuristic demonstration that, while not yielding superconvergence, provides insight into why one might anticipate  $I_1$  to be of order  $t^4$ . Consider the expression

$$A(t) = \alpha + \beta t + \gamma t^2, \quad (51)$$

where  $\alpha$ ,  $\beta$  and  $\gamma$  are all independent of the time  $t$ . A straightforward calculation reveals that the  $t^3$  contributions, arising only from terms like  $[\alpha, [\alpha, \beta]]$ , exactly cancel out. The leading-order terms are of order  $t^4$  and are associated with  $[\beta, [\alpha, \beta]]$  and  $[\alpha, [\alpha, \gamma]]$ .

Despite this observation, it is crucial to emphasize that this does *not* lead to superconvergence. This is primarily because superconvergence not only requires a  $t^4$  estimate, but more importantly, it demands the preconstant to be bounded solely by the nature of  $B$ . When  $t$  is not sufficiently small (in this case, as small as  $1/\|A\|$ ), the higher-order terms in the Taylor expansion cease to remain controlled. To elaborate further, the interaction depicted as  $A(t) = -ie^{iAt}Be^{-iAt}$  does not conform to the simple form of Eq. (51). Instead, it can be expressed as:

$$A(t) = -iB + [A, B]t + i \int_0^t d\sigma e^{i(t-\sigma)A} [A, [A, B]] e^{-i(t-\sigma)A} := \alpha + \beta t + \gamma(t), \quad (52)$$

where  $rt^3$  is replaced by  $r(t)$ , preventing a perfect cancellation of the  $t^3$  terms. This leads to terms that are challenging to control, for instance:

$$[\alpha, [\beta, \gamma(t)]]t^3 = [\alpha, [\beta, A(t) - \alpha - \beta t]]t^3 = [\alpha, [\beta, A(t)]]t^3. \quad (53)$$

Here we leverage the fact that  $[\alpha, [\beta, \alpha]] \sim [V(x), [\partial_x^2, V(x)], V(x)] = 0$ , where  $\sim$  denotes equality up to an absolute constant. To achieve superconvergence, Eq. (53) needs to be bounded by  $Ct^4$ , necessitating the bounding of  $\|[\alpha, [\beta, A(t)]]\|$  by  $Ct$  with some  $C$  depending only on  $B$  and independent of the number of grids  $N$ . Unfortunately, this is not the case. As evidenced by Fig. 1a, where the term can be linearly bounded in  $t$  but with a constant dependent on the number of grids  $N$ . Other terms associated with  $\gamma(t)$  can be even more challenging to estimate, for example, one needs to prove that  $\|[\gamma(s), [\alpha, \gamma(t)]]\| \leq Ct^3$ .

Furthermore, expanding  $A(t)$  for one more order does not alleviate these difficulties, and similar challenges arise in the remainder term. The key takeaway is that Taylor expansions or Taylor theorem-style estimates fail to account for the destructive interference resulting from integrals and the cohesive behavior of multiple terms. A naive but inaccurate analogy is to consider how  $e^{-iHt}$  remains bounded even for unbounded  $H$  (the bound is independent of the norm of  $H$ ). However, once one expands it in its Taylor series and attempts to estimate, one ends up with a bound that depends on the norms of  $H$ , which can become infinity for unbounded operators. This aligns with the observation of the superconvergence result for the first-order Magnus truncation [43]. To address such interference and achieve an improved estimate, we pursue the route of pseudodifferential operators in the next section.

## 4.2 Rigorous proof of superconvergence

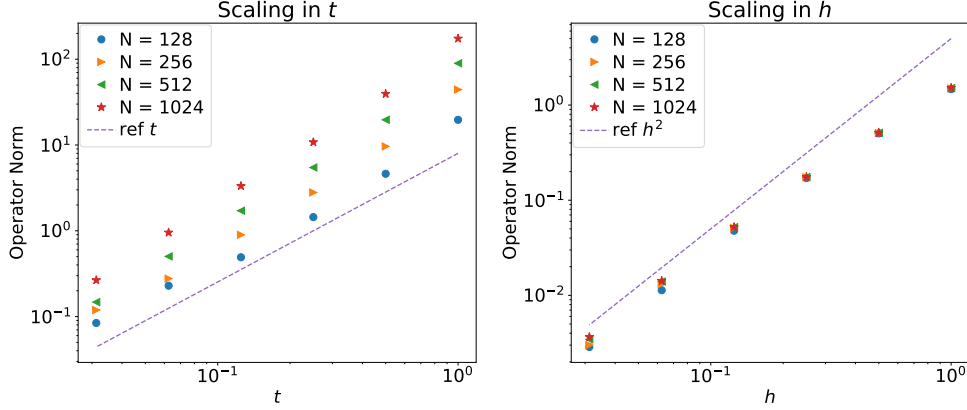
In this section, we aim to provide the crucial estimate to establish the superconvergence in the case of the unbounded Hamiltonian simulation, in particular,  $A = \Delta$  represents the Laplacian operator and  $B = V(x)$ . We start by considering an estimate of  $I_1$  as defined in Eq. (23).

The following trivial yet useful fact can come in handy in simplifying the terms.

$$[e^{iAs} B e^{-iAs}, e^{iAt} C e^{-iAt}] = e^{iAt} [e^{iA(s-t)} B e^{-iA(s-t)}, C] e^{-iAt}. \quad (54)$$

It immediately follows that

$$\begin{aligned} [A(\tau), [A(s), A(t)]] &= i \left[ e^{iA\tau} B e^{-iA\tau}, e^{iAt} [e^{iA(s-t)} B e^{-iA(s-t)}, B] e^{-iAt} \right] \\ &= i e^{iAt} \left[ e^{iA(\tau-t)} B e^{-iA(\tau-t)}, [e^{iA(s-t)} B e^{-iA(s-t)}, B] \right] e^{-iAt}. \end{aligned}$$



(a) Operator norm of a term in Taylor expansion (b) Operator norm of the key commutator

Figure 1: The unbounded Hamiltonian simulation problem considers the Hamiltonian  $-\Delta + \cos(x)$ , and  $A$  and  $B$  are the central finite discretization of the operators  $-\Delta$  and  $\cos(x)$  respectively with periodic boundary conditions using  $N$  spatial grids. Left: Plot of the operator norm of the term  $[\alpha, [\beta, \gamma(t)]]$  versus the short time  $t \in [0, 1]$  for various grid numbers  $N$ . This serves as evidence for terms becoming uncontrolled when expanding in the Taylor form. Right: Plot of the operator norm of the key commutator as in Lemma 5. This demonstrates that the key commutator remains controlled, insensitive to the grid number  $N$ , in contrast to the term after expanding by Taylor theorems. The numerical evidence agrees with the theoretical result proved in Lemma 5.

Thus it suffices to show that

$$\sup_{\tau, s \in [-h, h]} \left\| [e^{iA\tau} B e^{-iA\tau}, [e^{iAs} B e^{-iAs}, B]] \right\| \leq C_B h^2, \quad (55)$$

where  $C_B$  only depends on the potential  $V$  and its derivatives. If that is the case, then we have  $\|I_1\| \leq C_B h^4$ , where the additional two powers of  $h$  arise from the double layer integrals over the time interval  $[t, t + h]$ . This is precisely what we are able to establish in the case of unbounded Hamiltonian simulation, where  $A = \Delta$  represents the Laplacian operator and  $B = V(x)$  is the potential under certain assumptions. The proof relies on a careful analysis of the pseudodifferential operators, as detailed in Appendix A.

**Lemma 5** (The key commutator estimate). *Let  $V \in C^\infty(\mathbb{R}^d)$  bounded together with all of its derivatives. Then for every  $0 \leq h \leq 1$  we have*

$$\sup_{\tau, s \in [-h, h]} \left\| [e^{i\Delta\tau} V(x) e^{-i\Delta\tau}, [e^{i\Delta s} V(x) e^{-i\Delta s}, V(x)]] \right\|_{\mathcal{L}(L^2)} \leq C_V h^2, \quad (56)$$

where  $C_V$  is some constant depending only on  $V$  and the dimension  $d$ .

*Proof.* The proof follows by setting  $h_0 = 1$  in Lemma 18, proved in Appendix A.  $\square$

We now address the terms  $I_3$  and  $I_2$ . Although  $I_3$  comprises eight terms, they are easy to bound since each term involves at least three layers of time integrals and at least three layers of nested

commutators in terms of  $A(t)$ . Utilizing Eq. (54), we have

$$\| [A(t), A(s)] \| = \left\| [e^{iA(s-t)} B e^{-iA(s-t)}, B] \right\|. \quad (57)$$

The estimate of the right-hand side is proved in [43, Lemma 10] as follows:

**Lemma 6.** *For a smooth function  $V$  bounded together with all of its derivatives and  $0 < h \leq 1$ , we have*

$$\max_{s \in [-h, h]} \left\| [V(x), e^{is\Delta} V(x) e^{-is\Delta}] \right\|_{\mathcal{L}(L^2)} \leq C_V h, \quad (58)$$

where  $C_V$  is some constant depending only on  $V$  and the dimension  $d$ .

Moreover, note that  $\|A(t)\| = \|B\|$  depends only on  $V$ , and three layers of time integrals contribute to  $t^3$  or equivalently  $h^3$  for  $t \in [-h, h]$ . Hence, we have  $\|I_3\| \leq Ch^4$ , with some constant  $C$  depending only on  $V$ . Additionally,  $I_2 = g(\text{ad}_{\Omega_2})(\text{ad}_{\Omega_2}^3(\dot{\Omega}_2))$  follows a similar argument, as  $\text{ad}_{\Omega_2}^3(\dot{\Omega}_2)$  contains at least three layers of time integrals and three layers of nested commutators. We can state the following lemma, which is a direct consequence of the Magnus series expansion. We have provided the proof in Appendix B for completeness.

**Lemma 7.** *For  $\Omega_2$  and  $g$  defined in Eq. (10) and Eq. (21), we have*

$$\left\| g(\text{ad}_{\Omega_2})(\text{ad}_{\Omega_2}^3(\dot{\Omega}_2)) \right\| \leq C \left\| \text{ad}_{\Omega_2}^3(\dot{\Omega}_2) \right\|, \quad (59)$$

where  $C$  is some absolute constant.

We comment that this immediately implies that

$$\|I_2\| \leq 2C \sup_{t \in [-h, h]} \|\Omega_2\| \left\| \text{ad}_{\Omega_2}^2(\dot{\Omega}_2) \right\| \leq C_V h^5, \quad (60)$$

where  $C_V$  depends only on  $V$ . The last inequality follows from the fact that  $\text{ad}_{\Omega_2}^2(\dot{\Omega}_2)$  contains the terms in  $I_1$  and  $I_3$  that we have already estimated.

Combining the estimates of  $I_1$ ,  $I_2$ , and  $I_3$ , we have the following theorem.

**Theorem 8** (Superconvergence of Unbounded Hamiltonian Simulation). *For the exact propagator  $U_{\text{exact}}(t, s) = \mathcal{T} \exp\left(-i \int_s^t H(s) ds\right)$  and the second-order Magnus truncation  $U_2(t, s) := e^{\Omega_2(t, s)}$ , where  $\Omega_2(t, s)$  is defined as Eq. (14), we have*

$$\|U_{\text{exact}}(t_{j+1}, t_j) - U_2(t_{j+1}, t_j)\| \leq C_V h^5, \quad (61)$$

for some constant  $C_V$  depending only on  $V$  and the dimension  $d$ .

This implies for the long-time evolution over  $[0, T]$ , the error is bounded by  $C_V T h^4$  so that the algorithm is fourth order.

## 5 Circuit construction

In this section, we first discuss the construction of quantum circuits for dynamical simulation with our algorithm based on the second-order Magnus series truncation. With access to the input model of the time-dependent Hamiltonian in the Schrödinger picture or interaction picture, we discuss the complexity of long-time dynamical simulation with second-order Magnus expansion. In particular, we demonstrate that long-time quantum dynamics simulation can be implemented with second-order-Magnus series and superconvergence can be achieved.

## 5.1 Input model

The input model refers to the oracle in the quantum circuit giving access to the Hamiltonian of interests. Building an input model for a quantum system is a necessary step before constructing the numerical scheme, for example, quantum signal processing, on quantum computers. Block Encoding is one general framework used to construct an input model on fault-tolerant quantum computer [63, 64]. It has been developed for a number of operators including sparse matrices [65], pseudo-differential operator [66] as well as quantum many-body Hamiltonian [67–70].

### 5.1.1 Input model for $H(t)$

In this work, we adopt the same input model as used in [20]. Assume we are provided with the unitary oracle HAM-T, which encodes the Hamiltonian evaluated at different discrete time steps. Specifically, given a time-dependent Hamiltonian  $H(t)$  with  $\|H(t)\| \leq \alpha$ , two non-negative integers  $j, M$ , and a time step size  $h$ , let HAM-T $_j$  be an  $(n_s+n_a+n_m)$ -qubit unitary oracle with  $n_m = \log_2 M$  such that

$$\langle 0^{n_a} | \text{HAM-T}_j | 0^{n_a} \rangle = \sum_{k=0}^{M-1} |k\rangle \langle k| \otimes \frac{H(jh + kh/M)}{\alpha}. \quad (62)$$

Here  $M$  is the number of quadrature points used in numerical quadrature,  $j$  is the current local time step,  $h$  is the time step size in the time discretization, and  $n_s, n_a$  denote the number of the state space qubits and ancilla qubits, respectively.

### 5.1.2 Input model for interaction picture

We assume access to a fast-forwarded Hamiltonian simulation subroutine for the matrix  $A$  and the HAM-T oracle for  $B(t)$ , namely:

1.  $O_A(s)$  which can fast-forward  $e^{iAs}$  for any  $s \in \mathbb{R}$ .
2.  $O_B(j)$ , which is the HAM-T oracle for  $B(t)$  on the interval  $[jh, (j+1)h]$ , i.e., an  $(n_s+n_B+n_m)$ -qubit unitary oracle with  $n_m = \log_2 M$  and  $n_B$  denoting the number of ancilla qubits such that

$$\langle 0^{n_B} | O_B(j) | 0^{n_B} \rangle = \sum_{k=0}^{M-1} |k\rangle \langle k| \otimes \frac{B(jh + kh/M)}{\alpha_B}. \quad (63)$$

Here  $\alpha_B$  is the block-encoding factor such that  $\max_{t \in [0, T]} \|B(t)\| \leq \alpha_B$ .

## 5.2 Quantum circuit for second-order Magnus expansion

The unitary  $\tilde{U}_2$  defined in Eq. (40) can be implemented on a quantum computer by the linear combination of unitary (LCU) [71, 72] with HAM-T as an input model and the quantum singular value transformation (QSVT) [63]. One way to further implement (16) is to use the quantum circuit to block encodes multiplications of each  $\tilde{U}_2$  operator (See [63] for details). An alternative approach is to block encode the full exponential factor in Eq. (16) and apply QSVT in the end. Both methods require a technique named oblivious amplitude amplification (OAA) to improve the final success probability of post-selection of correct dynamical simulation after block encoding. In this section, we mainly focus on the construction of a short-time evolution operator  $\tilde{U}(t_j, t_{j+1})$  for

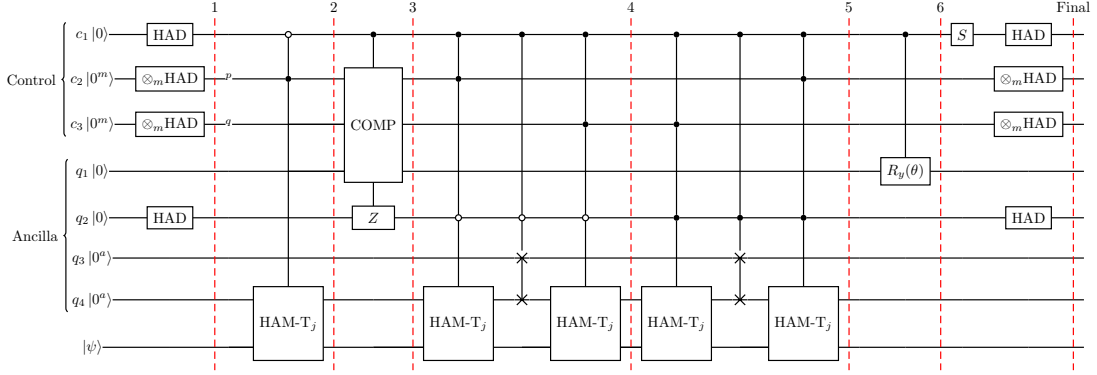


Figure 2: Quantum circuit of implementing the block-encoding of the Hamiltonian of the second-order Magnus expansion for general Hamiltonian Eq. (65). The short-time evolution operator can then be implemented according to Lemma 11 using the circuit here as input block encoding of Hamiltonian. Here HAD is the single qubit Hadamard gate and COMP is a compare oracle defined in Eq. (64). The HAM-T<sub>j</sub> is the input model for the time-dependent Hamiltonian at the time step. For the readability of superscripts and subscripts, we use  $a$  and  $m$  to represent  $n_a$  and  $n_m$  respectively in this figure.

our algorithm based on the second-order Magnus expansion, and the long-time evolution operator can be constructed afterward.

To implement the double integral in the second-order Magnus expansion, we use a COMP oracle such that,

$$\text{COMP } |p\rangle |q\rangle |0\rangle = \begin{cases} |p\rangle |q\rangle |0\rangle & \text{if } q < p \\ |p\rangle |q\rangle |1\rangle & \text{otherwise,} \end{cases} \quad (64)$$

to control the range of integral. The COMP oracle has been developed and used for a number of applications including state preparation [73]. The idea of such COMP oracle lies in comparing the binary representation of two integers from the most significant bits to less important bits [74] and we apply the COMP oracle with mid-circuit measurement to reduce the number of ancilla qubits needed [75].

We implement the Hamiltonian of the short time evolution operator from second-order Magnus expansion in Figure 2. The Hamiltonian of the second-order Magnus expansion can be decomposed into the summation of two Hamiltonians, corresponding to first-order and second-order expansion terms of the Magnus series. We use a control qubit  $c_1$  and LCU to construct the summation of two terms in Eq. (40). For the first order term, we use LCU approach and HAM-T oracle to construct a linear combination of  $H(t)$  for different  $t \in [t_j, t_j + 1]$ . The second order term  $\frac{1}{2}[H(t_j + \frac{q\hbar}{M}), H(t_j + \frac{p\hbar}{M})]$  is constructed through a LCU and a Pauli Z gate. The LCU technique contributes to the summation of the commutator and  $\frac{1}{2}$  and Z gate contribute to the minus sign in the commutator.

To be more precise about how the circuit works, we verify the evolution of wave-state vector  $\psi$  under the quantum circuit and prove it is a block encoding of second-order Magnus expansion.



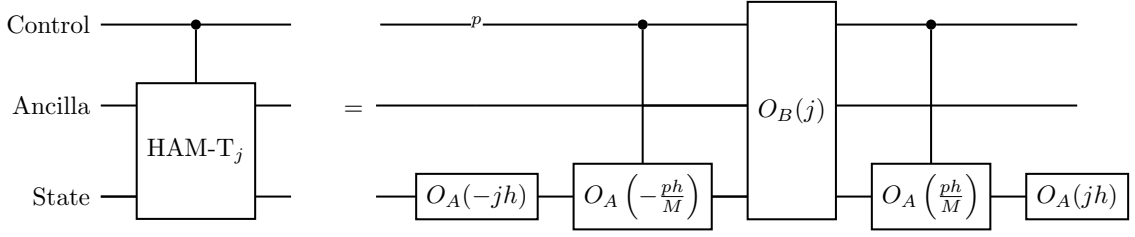


Figure 3: Quantum circuit of the HAM-T oracle in the interaction picture Hamiltonian for  $H(t) = A + B(t)$ .

**Lemma 9.** *Quantum circuit illustrated in Fig. 2 is a  $(2\alpha h, n_s + 2n_m + 2n_a + 3, 0)$  block encoding of Hamiltonian  $H$  derived from second-order Magnus series truncation with time discretization,*

$$\sum_{p=0}^{M-1} H(t_j + \frac{ph}{M}) \frac{h}{M} + \frac{i}{2} \sum_{p=0}^{M-1} \left[ \sum_{q=0}^{p-1} H(t_j + \frac{qh}{M}) \frac{h}{M}, H(t_j + \frac{ph}{M}) \right] \frac{h}{M}, \quad (65)$$

defined in Eq. (40) for the short time interval  $[t_j, t_{j+1}]$ .

*Proof.* Assume we start with state  $|0^{2n_m+2n_a+3}\rangle |\psi\rangle$  where  $\psi$  represents a  $n_s$ -qubit state. Then the circuit gives

$$\begin{aligned} & |0^{2n_m+2n_a+3}\rangle |\psi\rangle \xrightarrow{\text{Step1}} \frac{1}{2M} \sum_{i=0}^1 |i\rangle \sum_{p,q=0}^{M-1} |p\rangle |q\rangle |0\rangle \sum_{k=0}^1 |k\rangle |0^{2n_a}\rangle |\psi\rangle \\ & \xrightarrow{\text{Step2}} \frac{1}{2\alpha M} |0\rangle \sum_{p,q=0}^{M-1} |p\rangle |q\rangle |0\rangle \sum_{k=0}^1 |k\rangle |0^{2n_a}\rangle |H(t_j + \frac{ph}{M})\psi\rangle \\ & \quad + \frac{1}{2M} |1\rangle \sum_{p,q=0}^{M-1} |p\rangle |q\rangle |0\rangle \sum_{k=0}^1 |k\rangle |0^{2n_a}\rangle |\psi\rangle \\ & \xrightarrow{\text{Step3}} \frac{1}{2\alpha M} |0\rangle \sum_{p,q=0}^{M-1} |p\rangle |q\rangle |0\rangle \sum_{k=0}^1 |k\rangle |0^{2n_a}\rangle |H(t_j + \frac{ph}{M})\psi\rangle \\ & \quad + \frac{1}{2M} |1\rangle \sum_{q < p}^{M-1} |p\rangle |q\rangle |0\rangle (|0\rangle |0^{2n_a}\rangle |\psi\rangle - |1\rangle |0^{2n_a}\rangle |\psi\rangle) + |\Psi\rangle_{\text{drop}} \\ & \xrightarrow{\text{Step4}} \frac{1}{2\alpha M} |0\rangle \sum_{p,q=0}^{M-1} |p\rangle |q\rangle |0\rangle \sum_{k=0}^1 |k\rangle |0^{2n_a}\rangle |H(t_j + \frac{ph}{M})\psi\rangle \\ & \quad + \frac{1}{2M} |1\rangle \sum_{q < p}^{M-1} |p\rangle |q\rangle |0\rangle \left( \frac{1}{\alpha^2} |0\rangle |0^{2n_a}\rangle |H(t_j + \frac{qh}{M})H(t_j + \frac{ph}{M})\psi\rangle - |1\rangle |0^{2n_a}\rangle |\psi\rangle \right) + |\Psi\rangle_{\text{drop}} \end{aligned} \quad (66)$$

Step 1 diffuses the all-zero state to the superposition of states corresponding to the summation of first-order term and second-order term in the Hamiltonian. Step 2 is used to construct the first-order terms in the Hamiltonian. The second-order terms, i.e. the commutators, are constructed from step 3 to step 5 through LCU and a compare oracle.

$$\begin{aligned}
&\xrightarrow{\text{Step5}} \frac{1}{2\alpha M} |0\rangle \sum_{p,q=0}^{M-1} |p\rangle |q\rangle |0\rangle \sum_{k=0}^1 |k\rangle |0^{2n_a}\rangle |H(t_j + \frac{ph}{M})\psi\rangle \\
&\quad + \frac{1}{2\alpha^2 M} |1\rangle \sum_{q<p}^{M-1} |p\rangle |q\rangle |0\rangle \left( |0\rangle |0^{2n_a}\rangle |H(t_j + \frac{qh}{M})H(t_j + \frac{ph}{M})\psi\rangle - |1\rangle |0^{2n_a}\rangle |H(t_j + \frac{ph}{M})H(t_j + \frac{qh}{M})\psi\rangle \right) + |\Psi\rangle_{drop} \\
&\xrightarrow{\text{Step6}} \frac{1}{2\alpha M} |0\rangle \sum_{p,q=0}^{M-1} |p\rangle |q\rangle |0\rangle \sum_{k=0}^1 |k\rangle |0^{2n_a}\rangle |H(t_j + \frac{ph}{M})\psi\rangle \\
&\quad + \frac{h}{2\alpha M} |1\rangle \sum_{q<p}^{M-1} |p\rangle |q\rangle |0\rangle \left( |0\rangle |0^{2n_a}\rangle |H(t_j + \frac{qh}{M})H(t_j + \frac{ph}{M})\psi\rangle - |1\rangle |0^{2n_a}\rangle |H(t_j + \frac{ph}{M})H(t_j + \frac{qh}{M})\psi\rangle \right) + |\Psi\rangle_{drop} \\
&\xrightarrow{\text{End}} \frac{1}{2\alpha M} |0\rangle |0^{n_m}\rangle |0^{n_m}\rangle |0\rangle |0\rangle |0^{2a}\rangle \sum_{p=0}^{M-1} |H(t_j + \frac{ph}{M})\psi\rangle \\
&\quad + \frac{ih}{4\alpha M^2} |0\rangle |0^{n_m}\rangle |0^{n_m}\rangle |0\rangle \sum_{q<p}^{M-1} \left( |0\rangle |0^{2n_a}\rangle |H(t_j + \frac{qh}{M})H(t_j + \frac{ph}{M})\psi\rangle - |0\rangle |0^{2n_a}\rangle |H(t_j + \frac{ph}{M})H(t_j + \frac{qh}{M})\psi\rangle \right) + |\Psi\rangle_{drop}
\end{aligned} \tag{67}$$

After each step, we use the notation  $|\Psi\rangle_{drop}$  to denote the dropped term after post-selection. Although written in ket notation, we note that the state is not normalized and the notation may represent a different state in each step. For the post-selection, we measure all the control qubits and ancilla qubits. Only when all the measurement results are zero, we accept the output of the quantum circuit. In step 6, we use a control-rotation gate to adjust the coefficients and the rotation angle is,

$$\theta = \arccos(\alpha h). \tag{68}$$

The detailed derivation verifies the circuit is a  $(2\alpha h, 2n_m + 2n_a + 3, 0)$  block encoding of time discretization of second-order Magnus expansion.  $\square$

**Remark 10.** *The construction of COMP oracle requires two additional ancilla qubits but can be uncomputed, and we do not include the two qubits here.*

### 5.3 Long-time complexity of second-order Magnus expansion

In order to estimate the complexity of long-time quantum dynamics simulation through the second-order Magnus expansion, we start the section by recalling the following lemma [63] (see also [43, Lemma 2]).

**Lemma 11** (Time-independent Hamiltonian simulation via QSVT and OAA). *Let  $\epsilon \in (0, 1)$ ,  $t = \Omega(\epsilon)$  and let  $U$  be an  $(\alpha, n_a, 0)$ -block-encoding of a time-independent Hamiltonian  $H$ . Then*

a unitary  $V$  can be implemented such that  $V$  is a  $(1, n_a + 2, \epsilon)$ -block-encoding of  $e^{-itH}$ , with  $\mathcal{O}(\alpha t + \log(1/\epsilon))$  uses of  $U$ , its inverse or controlled version,  $\mathcal{O}(n_a(\alpha t + \log(1/\epsilon)))$  elementary gates and  $\mathcal{O}(1)$  additional ancilla qubits.

Lemma 9 and Lemma 11 contribute to the estimation of dynamical simulation cost with second-order Magnus expansion, summarized in the Theorem 12.

**Theorem 12** (Long-time complexity of Second-order Magnus expansion). *Let the Hamiltonian  $H(s)$  satisfies  $\|H(s)\| \leq \alpha$  for all  $0 \leq s \leq T$ . If*

$$\|U_{\text{exact}}(t_{j+1}, t_j) - U_2(t_{j+1}, t_j)\| \leq C_H h^{1+\theta}. \quad (69)$$

for a non-negative real number  $\theta$  and a constant  $C_H$  which might depend on  $H$ . Then for any  $0 < \epsilon < 1, T > \epsilon$ , our algorithm can implement an operation  $\exp(\tilde{\Omega}_2)$  such that  $\|W - U(T, 0)\| \leq \epsilon$  with failure probability  $\mathcal{O}(\epsilon)$  and the following cost:

1.  $\mathcal{O}\left(\alpha T + \frac{C_H^{1/\theta} T^{1+1/\theta}}{\epsilon^{1/\theta}} \log\left(\frac{C_H T}{\epsilon}\right)\right)$  uses of HAM- $T_j$ , its inverse or controlled version,
2.  $\mathcal{O}\left(\alpha T + \frac{C_H^{1/\theta} T^{1+1/\theta}}{\epsilon^{1/\theta}} \log\left(\frac{C_H T}{\epsilon}\right)\right)$  uses of COMP oracle or controlled version.
3.  $\mathcal{O}\left(\left(n_a + \log\left(\frac{\max_{s \in [0, T]} \|H'(s)\| T}{C_H \epsilon}\right)\right) \left(\alpha T + \frac{C_H^{1/\theta} T^{1+1/\theta}}{\epsilon^{1/\theta}} \log\left(\frac{C_H T}{\epsilon}\right)\right)\right)$  one- or two-qubit gates,
4.  $\mathcal{O}(1)$  additional ancilla qubits.

*Proof.* We start with Eq. (65) which is a  $(2\alpha h, n_s + 2n_a + 2n_m + 3, 0)$ -block-encoding of second order Magnus series in Eq. (65),

$$\sum_{p=0}^{M-1} H\left(t_j + \frac{ph}{M}\right) \frac{h}{M} + \frac{i}{2} \sum_{p=0}^{M-1} \left[ \sum_{q=0}^{p-1} H\left(t_j + \frac{qh}{M}\right) \frac{h}{M}, H\left(t_j + \frac{ph}{M}\right) \right] \frac{h}{M} \quad (70)$$

with five query to HAM- $T_j$  oracle, one query to COMP oracle,  $\mathcal{O}(n_m)$  single-qubit gates and two controlled-SWAP gates. According to Lemma 11, a  $(1, 2n_a + 2n_m + 5, \delta)$ -block-encoding of  $\tilde{U}_2(t_{j+1}, t_j)$  can be implemented by QSVT, with  $\mathcal{O}(2\alpha h + \log(1/\delta))$  uses of the block encoding for second-order Magnus expansion,  $\mathcal{O}((n_s + 2n_a + 2n_m + 3)(2\alpha h + \log(1/\delta)))$  elementary gates and  $\mathcal{O}(1)$  additional ancilla qubits. By setting

$$M = \mathcal{O}\left(\frac{\max_{s \in [0, T]} \|H'(s)\|}{C_H h^{\theta-1}}\right), \quad (71)$$

the implementation is a  $(1, n_s + 2n_a + 2n_m + 5, \delta')$ -block-encoding of  $U_2(t_{j+1}, t_j)$ , where

$$\delta' = \delta + 2C_H h^{\theta+1}. \quad (72)$$

Let  $V_j$  denote the circuit constructed in Fig. 2 and let  $n_b = 2n_a + 2n_m + 5$ , then we have for  $W_j = \langle 0|_b V_j |0\rangle_b$ ,

$$\|W_j - U_2(t_{j+1}, t_j)\| \leq \delta'. \quad (73)$$

With  $\|W_j\| \leq 1$  and  $\|U(t_{j+1}, t_j)\|$ , we have

$$\|\Pi_{j=0}^{L-1} W_j - U(T, 0)\| \leq L\delta'. \quad (74)$$

The success probability of evolving the state  $\psi$ , then can be estimated as

$$\|(\langle 0|_b \otimes I_{n_s}) \Pi_{j=0}^{L-1} V_j |0\rangle_b |\psi\rangle\| \quad (75)$$

where  $I_{n_s}$  denotes the identity operator on the  $n_s$  qubits. Since  $\|W_j - U_2(t_{j+1}, t_j)\| \leq \delta'$ , the success probability of each step, is thus bounded by

$$1 - (1 - \delta')^2 < 2\delta'. \quad (76)$$

After  $L$  steps, the failure probability is bounded by

$$1 - (1 - 2\delta')^L \leq 2L\delta'. \quad (77)$$

To bound the total error below  $\mathcal{O}(\epsilon)$ , we require

$$L\delta' = L\delta + 2\frac{C_H T^{\theta+1}}{L^\theta} \leq 3\epsilon. \quad (78)$$

By bounding the first and second terms on the left side by  $\epsilon$  and  $2\epsilon$  respectively, it suffices to choose

$$L = \frac{C_H^{1/\theta} T^{1+1/\theta}}{\epsilon^{1/\theta}}, \quad \delta = \frac{\epsilon^{1+1/\theta}}{C_H^{1/\theta} T^{1+1/\theta}}, \quad (79)$$

and correspondingly

$$M = \mathcal{O}\left(\frac{\max_{s \in [0, T]} \|H'(s)\| T^{1-1/\theta}}{C_H^{1/\theta} \epsilon^{1-1/\theta}}\right). \quad (80)$$

□

**Remark 13.** We note that the multi-qubit controlled HAM- $T_j$  is counted as a single query to HAM- $T_j$ . For a clear illustration of the circuit logic, we put the qubit  $c_1$  to the top and there could be additional cost due to long-range control for controlled-SWAP gate or controlled-Z gate. However, in real implementation, the cost can be removed as the qubit  $c_1$  can be moved to the middle of  $c_3$  and  $q_1$ .

We summarize the query complexity of the input model for simulating long-time quantum dynamics with second-order Magnus expansion for both general  $H$  and the interaction picture with superconvergence in Table 1. Note that although the scaling of the derivative bound and superconvergence appear similar, it is important to note that for unbounded Hamiltonian simulation,  $C_V$  in the superconvergence result is  $N$  independent, while  $C'_H$  depends on  $N$  polynomially, where  $N$  is the number of spatial grids.

General $H$	$\mathcal{O}\left(\alpha T + \frac{C_{\text{comm}}^{1/2} T^{3/2}}{\epsilon^{1/2}} \log\left(\frac{C_{\text{comm}} T}{\epsilon}\right)\right)$
General $H$ with derivative bound	$\mathcal{O}\left(\alpha T + \frac{(C'_H)^{1/4} T^{5/4}}{\epsilon^{1/4}} \log\left(\frac{C'_H T}{\epsilon}\right)\right)$
Superconvergence	$\mathcal{O}\left(\alpha_B T + \frac{C_V^{1/4} T^{5/4}}{\epsilon^{1/4}} \log\left(\frac{C_V T}{\epsilon}\right)\right)$

Table 1: Comparison of query complexities of long time dynamics simulation with second order Magnus series based on different assumptions of Hamiltonian  $H$ . For general Hamiltonian  $H$ , query complexities are measured by the number of queries to the input of the time-dependent Hamiltonian. For the interaction picture, the query complexity is measured with respect to the queries to the oracle  $e^{-iAt}$  or input model of  $B$ .

## 6 Conclusion and discussion

In this work, we develop a quantum algorithm based on the second-order Magnus expansion for general time-dependent Hamiltonian simulation problems. It has commutator scaling in the high-precision regime, and the cost is logarithmically dependent on the derivative of the underlying Hamiltonian, as our algorithm leverages a quadrature rule with many quadrature points and then implements it using an LCU-type circuit. Our algorithm functions similarly to a non-interpolatory Magnus integrator, meaning it avoids the errors typically induced by approximating the integral with only a few quadrature points. We further show that the algorithm is in general of second order. If one allows a polynomial dependence on the derivative, the algorithm can be of fourth order. Surprisingly, when the Hamiltonian simulation is taken to be the interaction picture of the unbounded Hamiltonian simulation for regular potentials, the algorithm exhibits a fourth-order superconvergence, where the error preconstant becomes only dependent on the potential  $V$ , making the overall gate cost only logarithmic dependent on  $N$ . This distinguishes our algorithm from other (classical) Magnus integrators that introduce polynomial derivative dependence of the Hamiltonian.

So far, the direct implementation of the Magnus expansion for general time-dependent Hamiltonians has been developed only for expansions up to the second order. In theory, the approach of truncating the Magnus series to a finite order and then implementing many quadrature points for the integrals via a suitable LCU-type circuit could be applied to arbitrarily high-order truncations. However, challenges can arise in both the circuit construction and the superconvergence proof. Exploring both challenges will be interesting future directions.

For the circuit, we implement the second-order Magnus expansion with a compare oracle to post-select the terms satisfying  $q < p$  in Eq. (40). Each register representing  $p$  or  $q$  requires  $\mathcal{O}(\log(\frac{T}{\epsilon}))$  qubits and the commutator is constructed with LCU techniques requiring one additional ancilla qubit. Direct generalization is less efficient as  $k$ -th order Magnus series requires  $k$  qubits for the composition of  $k$  layers commutator and  $\mathcal{O}(k)$  qubits for registers controlling the ordering of time register. Construction of a compression gadget to deal with the two issues for optimal  $T$  gate depth or optimal  $T$  gate counts will be left for future directions.

Although we can confidently conjecture that the superconvergence behavior extends to generalizations of our algorithms for high-order Magnus expansions, proving this for higher-order expansions presents substantial challenges. One clear reason is that we cannot rely on series expansions, such as the Taylor expansion. As we have seen, the superconvergence proof for the second-order Magnus expansion already involves 11 terms. Nevertheless, our proof highlights the cancellation mechanism through semiclassical analysis and categorizes the terms into a few groups, providing

insights for the generalization to the arbitrary higher-order scenario. Another interesting direction would be to seek other systems that can make better use of this type of commutator scaling and explore whether the superconvergence behavior exists for other physically motivated Hamiltonians.

## Acknowledgments

The authors would like to thank Prof. András Vasy for discussions on semiclassical microlocal analysis that led to the proof of Lemma 18. This material is based upon work supported by National Science Foundation via the grant DMS-2347791 (D.F.), DMREF Award No. 1922165, Simons Targeted Grant Award No. 896630 and Willard Miller Jr. Fellowship (D.L.), and the National Science Foundation via award number 1953987 (R.S.). We thank the Institute for Pure and Applied Mathematics (IPAM) for hosting all authors as long-term participants during the semester-long program “Mathematical and Computational Challenges in Quantum Computing” in Fall 2023, during which this work was initiated.

## A Proof of the key commutator estimate

The goal of this section is to prove Lemma 18, from which Lemma 6 follows as a special case. The proof uses standard results from semiclassical analysis [76, Chapter 4], and the result is an immediate consequence of these general results. We also give some necessary background for the ease of the reader. All functions will be complex-valued.

For any  $m \in \mathbb{R}$ , we begin by defining the symbol class  $S_{3n}(\langle p \rangle^m)$ , where  $\langle p \rangle = (1 + |p|^2)^{\frac{1}{2}}$ , and the reader should consult [76, Chapter 4] and [77, Chapter 2] for more information. Here the subscript  $3n$  corresponds to three copies of  $\mathbb{R}^n$ , which we will denote as  $\mathbb{R}_x^n, \mathbb{R}_y^n, \mathbb{R}_p^n$ , for reasons that will become clear below. For some  $h_0 > 0$  (which we will think of as fixed), the definition of  $S_{3n}(\langle p \rangle^m)$  is now as follows:

$$S_{3n}(\langle p \rangle^m) := \{a \in C^\infty(\mathbb{R}_x^n \times \mathbb{R}_y^n \times \mathbb{R}_p^n \times (0, h_0]_h) : \sup_{\mathbb{R}^{3n} \times (0, h_0]_h} |\langle p \rangle^{-m} (\partial_x^\alpha \partial_y^\beta \partial_p^\gamma a)(x, y, p, h)| \leq C_{\alpha, \beta, \gamma} < \infty\}, \quad (81)$$

that is the space of all smooth functions on  $\mathbb{R}^{3n} \times (0, h_0]_h$ , which are bounded together with all derivatives with respect to  $x, y, p$  after scaling by  $\langle p \rangle^{-m}$ , and these bounds are uniform in  $h \in (0, h_0]$ . It is traditional in semiclassical analysis to hide the dependence of symbols  $a \in S_{3n}(\langle p \rangle^m)$  on  $h$  for the ease of notation, and we will adopt this convention and simply write  $a(x, y, p)$  with dependence on  $h$  implicit. Similarly, we also define the symbol class

$$S_{2n}(\langle p \rangle^m) := \{a \in C^\infty(\mathbb{R}_x^n \times \mathbb{R}_p^n \times (0, h_0]_h) : \sup_{\mathbb{R}^{2n} \times (0, h_0]_h} |\langle p \rangle^{-m} (\partial_x^\alpha \partial_p^\gamma a)(x, p, h)| \leq C_{\alpha, \gamma} < \infty\}. \quad (82)$$

In (81) and (82),  $\alpha, \beta, \gamma$  are multi-indices. For the special case  $m = 0$ , we will denote the corresponding symbol classes as simply  $S_{3n}(1)$  and  $S_{2n}(1)$ . Let us now introduce semiclassical pseudodifferential operators defined by the (semiclassical) quantization of symbols in  $S_{3n}(\langle p \rangle^m)$ . For any  $h \in (0, h_0]$  and  $a \in S_{3n}(\langle p \rangle^m)$ , we define the quantization of  $a$  to be

$$\text{Op}_h(a) := \frac{1}{(2\pi h)^n} \int_{\mathbb{R}^n} a(x, y, p) e^{\frac{i}{h}(x-y) \cdot p} dp. \quad (83)$$

We also define the Weyl quantization of symbols in  $S_{2n}(\langle p \rangle^m)$ : if  $a \in S_{2n}(\langle p \rangle^m)$ , then it gives rise to a semiclassical pseudodifferential operator

$$\text{Op}_h^w(a) := \frac{1}{(2\pi h)^n} \int_{\mathbb{R}^n} a\left(\frac{x+y}{2}, p\right) e^{\frac{i}{h}(x-y)\cdot p} dp. \quad (84)$$

Formally the expressions in (83) and (84) define the Schwartz kernels of the corresponding pseudodifferential operators, which are oscillatory integral distributions.

As preparation for our proof, we will also need to restate some of the calculations done in the proof of [43, Lemma 10], but using semiclassical quantization. In particular, we note the following result, the proof of which follows using similar calculations as in [43] (we omit the proof):

**Lemma 14** (Weyl quantization formulas). *Let  $V \in C^\infty(\mathbb{R}_x^n)$ , such that  $V$  is bounded with all derivatives. Let us also assume that  $a \in S_{2n}(1)$ , and  $h \in (0, h_0]$ . Then we have the following:*

- (i) *We have the equality  $[\Delta, \text{Op}_h^w(a)] = \frac{2i}{h} \text{Op}_h^w\left(\sum_{i=1}^n p_i \frac{\partial a}{\partial x_i}\right)$ , where  $\sum_{i=1}^n p_i \frac{\partial a}{\partial x_i} \in S_{2n}(\langle p \rangle)$ .*
- (ii) *For all  $s \in \mathbb{R}$ , we have  $e^{ish\Delta} V e^{-ish\Delta} = \text{Op}_h^w(V(x - 2ps))$ , where  $(V(x - 2ps)) \in S_{2n}(1)$ , and does not depend on  $h$ .*

Using the above facts, the proof of Lemma 18 will follow using two standard results in semiclassical analysis. We begin by stating these results below.

**Lemma 15** (Semiclassical commutator, [77, Theorem 2.7.4, Remark 2.7.6]). *Let  $a, b \in S_{2n}(1)$ , and let  $\text{Op}_h^w(a)$  and  $\text{Op}_h^w(b)$  denote their Weyl quantizations. Then*

- (i) *There exists  $c, \tilde{c} \in S_{2n}(1)$  such that  $\text{Op}_h^w(a)\text{Op}_h^w(b) = \text{Op}_h^w(c)$ , and we can write  $c$  as*

$$\begin{aligned} c &= ab + \frac{h}{2i}\{a, b\} + h^2\tilde{c}, \\ \{a, b\} &:= \sum_{j=1}^n \left( \frac{\partial a}{\partial p_j} \frac{\partial b}{\partial x_j} - \frac{\partial a}{\partial x_j} \frac{\partial b}{\partial p_j} \right). \end{aligned} \quad (85)$$

- (ii) *For the commutator  $[\text{Op}_h^w(a), \text{Op}_h^w(b)]$ , there exists a symbol  $c \in S_{2n}(1)$  such that*

$$[\text{Op}_h^w(a), \text{Op}_h^w(b)] = \frac{h}{i} \text{Op}_h^w(\{a, b\}) + h^3 \text{Op}_h^w(c). \quad (86)$$

**Lemma 16** (Calderón-Vaillancourt, [77, Theorem 2.8.1]). *If  $a \in S_{3n}(1)$ , then  $\text{Op}_h(a)$  defines a continuous linear map from  $L^2(\mathbb{R}_y^n)$  to  $L^2(\mathbb{R}_x^n)$ . In particular, we have*

$$\|\text{Op}_h(a)\|_{L^2 \rightarrow L^2} \leq C_n \left( \sum_{|\alpha| \leq M_n} \sup_{(x,y,p) \in \mathbb{R}^{3n}} |\partial^\alpha a(x, y, p)| \right), \quad (87)$$

where the constants  $C_n$  and  $M_n$  depend only on  $n$ .

We next prove another important lemma that we will need:

**Lemma 17.** *Let  $V \in C^\infty(\mathbb{R}_x^n)$  such that  $V$  is bounded together with all its derivatives. Then we have the following:*

- (i) *If  $s \in [-h_0, h_0]$ , then there exists  $a \in S_{2n}(1)$ , such that  $[e^{i\Delta s} V e^{-i\Delta s}, V] = s \text{Op}_{|s|}^w(a)$ .*
- (ii) *Assume that  $s, \tau \in [-h, h]$  for some  $h \in (0, h_0]$ . Let  $s = rh$ ,  $\tau = qh$ . Then there exists  $a_{r,q} \in S_{2n}(1)$ , depending continuously on the parameters  $r, q \in [-1, 1]$ , such that*

$$[e^{i\Delta \tau} V e^{-i\Delta \tau}, [e^{i\Delta s} V e^{-i\Delta s}, V]] = h^2 \text{Op}_h^w(a_{r,q}). \quad (88)$$

*Proof.* For this proof, note that the assumptions on  $V$  ensure that  $V \in S_{2n}(1)$ .

- (i) For  $s = 0$ , we have  $[e^{i\Delta s} V e^{-i\Delta s}, V] = 0$ ; so let us assume that  $0 \neq s = th_0$ , for some  $t$ . Then from Lemma 14(ii), we have

$$e^{is\Delta} V e^{-is\Delta} = e^{ith_0\Delta} V e^{-ith_0\Delta} = \text{Op}_{h_0}^w(V(x - 2pt)). \quad (89)$$

Now, for  $t > 0$ , a simple variable change  $pt \mapsto p$  shows that we have

$$e^{is\Delta} V e^{-is\Delta} = \text{Op}_{h_0}^w(V(x - 2pt)) = \text{Op}_{th_0}^w(V(x - 2p)) = \text{Op}_s^w(V(x - 2p)), \quad (90)$$

where  $V(x - 2p) \in S_{2n}(1)$ . The importance of the above equation is that we have managed to make the symbol  $V(x - 2p)$  independent of  $t$ . Next using the fact that  $V = \text{Op}_s^w(V)$ , it immediately follows from Lemma 15 that there exists  $c \in S_{2n}(1)$  such that

$$\begin{aligned} [e^{i\Delta s} V e^{-i\Delta s}, V] &= [\text{Op}_s^w(V(x - 2p)), \text{Op}_s^w(V)] = \frac{s}{i} \text{Op}_s^w(b) + s^3 \text{Op}_s^w(c) = s \text{Op}_s^w\left(\frac{b}{i} + s^2 c\right), \\ b(x, p) &:= -2(\nabla V)(x - 2p) \cdot (\nabla V)(x). \end{aligned} \quad (91)$$

It follows that  $b \in S_{2n}(1)$ , as  $V \in S_{2n}(1)$ , and thus  $(b/i + s^2 c) \in S_{2n}(1)$  also. Finally, the case  $t < 0$  is similar and follows after performing the variable change  $-pt \mapsto p$ .

- (ii) We have  $e^{is\Delta} V e^{-is\Delta} = \text{Op}_h^w(V(x - 2pr))$ , and  $e^{i\tau\Delta} V e^{-i\tau\Delta} = \text{Op}_h^w(V(x - 2pq))$ , from Lemma 14(ii). Next we express the commutator  $[e^{is\Delta} V e^{-is\Delta}, V]$  using Lemma 15(ii) as

$$[e^{is\Delta} V e^{-is\Delta}, V] = [\text{Op}_h^w(V(x - 2pr)), \text{Op}_h^w(V)] = h \text{Op}_h^w\left(\frac{b_r}{i} + h^2 c_r\right), \quad (92)$$

where  $b_r, c_r \in S_{2n}(1)$ , with  $b_r(x, p) := -2r(\nabla V)(x - 2pr) \cdot (\nabla V)(x)$ , and also note that  $b_r, c_r$  depend continuously on  $r$ . Define  $\tilde{b}_r := b_r/i + h^2 c_r$ .

We can now calculate the commutator  $[e^{i\tau\Delta} V e^{-i\tau\Delta}, [e^{is\Delta} V e^{-is\Delta}, V]]$  the same way:

$$\begin{aligned} [e^{i\tau\Delta} V e^{-i\tau\Delta}, [e^{is\Delta} V e^{-is\Delta}, V]] &= [\text{Op}_h^w(V(x - 2pq)), h \text{Op}_h^w(\tilde{b}_r)] \\ &= h [\text{Op}_h^w(V(x - 2pq)), \text{Op}_h^w(\tilde{b}_r)] = h^2 (\text{Op}_h^w(d_{r,q}/i + h^2 f_{r,q})), \end{aligned} \quad (93)$$

where  $d_{r,q}, f_{r,q} \in S_{2n}(1)$  depend continuously on  $r, q$ , and

$$d_{r,q}(x, p) := -2q(\nabla V)(x - 2pq) \cdot (\nabla_x \tilde{b}_r)(x, p) + (\nabla V)(x - 2pq) \cdot (\nabla_p \tilde{b}_r)(x, p). \quad (94)$$

This completes the proof.



□

Note that part (i) of Lemma 17 can also be found in the proof of [43, Lemma 10], but we have derived the same fact using semiclassical tools. We are now ready to prove the main result of this appendix:

**Lemma 18.** *Let  $h_0 > 0$ , and  $V \in C^\infty(\mathbb{R}^n)$  bounded together with all of its derivatives. Then for every  $0 \leq h \leq h_0$  we have*

$$\sup_{\tau, s \in [-h, h]} \left\| [e^{i\Delta\tau} V e^{-i\Delta\tau}, [e^{i\Delta s} V e^{-i\Delta s}, V(x)]] \right\|_{L^2 \rightarrow L^2} \leq C_V h^2, \quad (95)$$

where  $C_V$  is some constant depending only on  $V$ ,  $n$ , and  $h_0$ .

*Proof.* Fix  $s, \tau \in [-h, h]$ , and suppose  $s = hr$ ,  $\tau = hq$ . Using Lemma 17(ii), we know that there exists  $a_{r,q} \in S_{2n}(1)$ , depending continuously on  $r, q \in [-1, 1]$ , such that  $[e^{i\Delta\tau} V e^{-i\Delta\tau}, [e^{i\Delta s} V e^{-i\Delta s}, V]] = h^2 \text{Op}_h^w(a_{r,q})$ . Now by Lemma 16, we have

$$\begin{aligned} & \left\| [e^{i\Delta\tau} V e^{-i\Delta\tau}, [e^{i\Delta s} V e^{-i\Delta s}, V]] \right\|_{L^2 \rightarrow L^2} = \left\| h^2 \text{Op}_h^w(a_{r,q}) \right\|_{L^2 \rightarrow L^2} \\ & \leq C_n h^2 \left( \sum_{|\alpha| \leq M_n} \sup_{(x,p) \in \mathbb{R}^{2n}} |\partial^\alpha a_{r,q}(x,p)| \right), \end{aligned} \quad (96)$$

where the constants  $C_n, M_n$  depend on the dimension  $n$  only. Now note that by continuity of  $a_{r,q}$  as a function of  $r, q$ , we know that the functions  $\sup_{(x,p) \in \mathbb{R}^{2n}} |\partial^\alpha a_{r,q}(x,p)|$  are also continuous functions of  $r, q \in [-1, 1]$ , for every multi-index  $\alpha$ . Finally, we take supremum over  $s, \tau \in [-h, h]$  of both sides of the above equation to get

$$\begin{aligned} & \sup_{\tau, s \in [-h, h]} \left\| [e^{i\Delta\tau} V e^{-i\Delta\tau}, [e^{i\Delta s} V e^{-i\Delta s}, V]] \right\|_{L^2 \rightarrow L^2} \\ & \leq C_n h^2 \left( \sum_{|\alpha| \leq M_n} \sup_{r, q \in [-1, 1]} \left( \sup_{(x,p) \in \mathbb{R}^{2n}} |\partial^\alpha a_{r,q}(x,p)| \right) \right) = C(n, V, h_0) h^2. \end{aligned} \quad (97)$$

The constant  $C(n, V, h_0)$  only depends on  $n$ , the potential function  $V$ , and implicitly on the parameter  $h_0$  (which we had fixed at the beginning). □

## B Proof of Lemma 7

*Proof of Lemma 7.* The proof of this lemma is fairly straightforward following [51, Lemma 5.1], where it is shown that  $g(z)$  has a Fourier transform  $\hat{g} \in L^1(\mathbb{R})$  defined as

$$g(ix) = \int_{\mathbb{R}} \hat{g}(\xi) e^{i\xi x} d\xi, \quad (98)$$

and its norm is bounded by some absolute constant

$$\|\hat{g}\|_{L^1(\mathbb{R})} \leq 2\pi \|g\|_{L^2(i\mathbb{R})}^{1/2} \|g'\|_{L^2(i\mathbb{R})}^{1/2}. \quad (99)$$

Plugging in the operators, one has

$$g(\text{ad}_{\Omega_2})(\text{ad}_{\dot{\Omega}_2}^3(\dot{\Omega}_2)) = \int_{\mathbb{R}} \hat{g}(\xi) e^{\text{ad}(\xi\Omega_2)} \text{ad}_{\dot{\Omega}_2}^3(\dot{\Omega}_2) d\xi = \int_{\mathbb{R}} \hat{g}(\xi) e^{\xi\Omega_2} \text{ad}_{\dot{\Omega}_2}^3(\dot{\Omega}_2) e^{-\xi\Omega_2} d\xi. \quad (100)$$

Note that  $\Omega_2$  is anti-Hermitian so that its exponential is unitary. Taking the norm of Eq. (100), we have

$$\left\| g(\text{ad}_{\Omega_2})(\text{ad}_{\dot{\Omega}_2}^3(\dot{\Omega}_2)) \right\| \leq \|\hat{g}\|_{L^1(\mathbb{R})} \left\| \text{ad}_{\dot{\Omega}_2}^3(\dot{\Omega}_2) \right\|. \quad (101)$$

□

## References

- [1] Richard P Feynman. Simulating physics with computers. *International Journal of Theoretical Physics*, 21(6):467–488, 1982.
- [2] Edward Farhi, Jeffrey Goldstone, Sam Gutmann, and Michael Sipser. Quantum computation by adiabatic evolution. 2000.
- [3] T. Albash and D. A. Lidar. Adiabatic quantum computation. *Rev. Mod. Phys.*, 90:015002, 2018.
- [4] Guang Hao Low and Isaac L. Chuang. Optimal Hamiltonian simulation by quantum signal processing. *Phys. Rev. Lett.*, 118:010501, 2017.
- [5] Guang Hao Low and Isaac L. Chuang. Hamiltonian simulation by qubitization. *Quantum*, 3:163, Jul 2019.
- [6] Andrew M. Childs, Yuan Su, Minh C. Tran, Nathan Wiebe, and Shuchen Zhu. Theory of trotter error with commutator scaling. *Phys. Rev. X*, 11:011020, 2021.
- [7] Lindsay Bassman Oftelie, Katherine Klymko, Diyi Liu, Norm M. Tubman, and Wibe A. de Jong. Computing free energies with fluctuation relations on quantum computers. *Phys. Rev. Lett.*, 129:130603, Sep 2022.
- [8] I. D. Kivlichan, N. Wiebe, R. Babbush, and A. Aspuru-Guzik. Bounding the costs of quantum simulation of many-body physics in real space. *J. Phys. A Math. Theor.*, 50:305301, 2017.
- [9] Rolando D. Somma. Quantum simulations of one dimensional quantum systems, 2015.
- [10] I.D. Kivlichan, J. McClean, N. Wiebe, C. Gidney, A. Aspuru-Guzik, G.K.-L. Chan, and R. Babbush. Quantum Simulation of Electronic Structure with Linear Depth and Connectivity. *Phys. Rev. Lett.*, 120(11):110501, 2018.
- [11] Dong An, Di Fang, and Lin Lin. Time-dependent unbounded Hamiltonian simulation with vector norm scaling. *Quantum*, 5:459, may 2021.
- [12] Yuan Su, Dominic W Berry, Nathan Wiebe, Nicholas Rubin, and Ryan Babbush. Fault-tolerant quantum simulations of chemistry in first quantization. *PRX Quantum*, 2(4):040332, 2021.

- [13] Andrew M. Childs, Jiaqi Leng, Tongyang Li, Jin-Peng Liu, and Chenyi Zhang. Quantum simulation of real-space dynamics, 2022.
- [14] Nicholas C. Rubin, Dominic W. Berry, Alina Kononov, Fionn D. Malone, Tanuj Khattar, Alec White, Joonho Lee, Hartmut Neven, Ryan Babbush, and Andrew D. Baczewski. Quantum computation of stopping power for inertial fusion target design, 2023.
- [15] Yu Tong, Victor V. Albert, Jarrod R. McClean, John Preskill, and Yuan Su. Provably accurate simulation of gauge theories and bosonic systems. *Quantum*, 6:816, September 2022.
- [16] Nilin Abrahamsen, Yu Tong, Ning Bao, Yuan Su, and Nathan Wiebe. Entanglement area law for one-dimensional gauge theories and bosonic systems. *Phys. Rev. A*, 108:042422, Oct 2023.
- [17] J. Mizrahi, B. Neyenhuis, K. G. Johnson, W. C. Campbell, C. Senko, D. Hayes, and C. Monroe. Quantum control of qubits and atomic motion using ultrafast laser pulses. *Applied Physics B*, 114(1-2):45–61, Nov 2013.
- [18] Michael A Nielsen, Mark R Dowling, Mile Gu, and Andrew C Doherty. Optimal control, geometry, and quantum computing. *Phys. Rev. A*, 73(6):062323, 2006.
- [19] Daoyi Dong and Ian R Petersen. Quantum control theory and applications: a survey. *IET Control Theory & Applications*, 4(12):2651–2671, 2010.
- [20] G. H. Low and N. Wiebe. Hamiltonian simulation in the interaction picture. 2019.
- [21] Abhishek Rajput, Alessandro Roggero, and Nathan Wiebe. Hybridized methods for quantum simulation in the interaction picture, 2021.
- [22] Chenyi Zhang, Jiaqi Leng, and Tongyang Li. Quantum algorithms for escaping from saddle points. *Quantum*, 5:529, August 2021.
- [23] Yizhou Liu, Weijie J. Su, and Tongyang Li. On quantum speedups for nonconvex optimization via quantum tunneling walks. *Quantum*, 7:1030, June 2023.
- [24] Jiaqi Leng, Ethan Hickman, Joseph Li, and Xiaodi Wu. Quantum hamiltonian descent, 2023.
- [25] Andrew M Childs and Yuan Su. Nearly optimal lattice simulation by product formulas. *Phys. Rev. Lett.*, 123(5):050503, 2019.
- [26] Burak Şahinoğlu and Rolando D Somma. Hamiltonian simulation in the low energy subspace. 2020.
- [27] Yuan Su, Hsin-Yuan Huang, and Earl T. Campbell. Nearly tight Trotterization of interacting electrons. *Quantum*, 5:495, July 2021.
- [28] Qi Zhao, You Zhou, Alexander F. Shaw, Tongyang Li, and Andrew M. Childs. Hamiltonian simulation with random inputs, 2021.
- [29] Di Fang and Albert Tres Vilanova. Observable error bounds of the time-splitting scheme for quantum-classical molecular dynamics. *SIAM J. Numer. Anal.*, 61(1):26–44, 2023.
- [30] Yonah Borns-Weil and Di Fang. Uniform observable error bounds of trotter formulae for the semiclassical schrödinger equation, 2022.

- [31] Pei Zeng, Jinzhao Sun, Liang Jiang, and Qi Zhao. Simple and high-precision hamiltonian simulation by compensating trotter error with linear combination of unitary operations, 2022.
- [32] Weiyuan Gong, Shuo Zhou, and Tongyang Li. A theory of digital quantum simulations in the low-energy subspace. *arXiv preprint arXiv:2312.08867*, 2023.
- [33] Guang Hao Low, Yuan Su, Yu Tong, and Minh C. Tran. Complexity of implementing trotter steps. *PRX Quantum*, 4:020323, May 2023.
- [34] Jacob Watkins, Nathan Wiebe, Alessandro Roggero, and Dean Lee. Time dependent hamiltonian simulation using discrete clock constructions, 2022.
- [35] Sergiy Zhuk, Niall Robertson, and Sergey Bravyi. Trotter error bounds and dynamic multi-product formulas for hamiltonian simulation, 2023.
- [36] Junaid Aftab, Dong An, and Konstantina Trivisa. Multi-product hamiltonian simulation with explicit commutator scaling, 2024.
- [37] J. Huyghebaert and H. De Raedt. Product formula methods for time-dependent Schrödinger problems. *J. Phys. A*, 23(24):5777–5793, 1990.
- [38] N. Wiebe, D. Berry, P. Høyer, and B. C. Sanders. Higher order decompositions of ordered operator exponentials. *J. Phys. A*, 43(6):065203, 2010.
- [39] D. W. Berry, A. M. Childs, R. Cleve, R. Kothari, and R. D. Somma. Simulating Hamiltonian dynamics with a truncated Taylor series. *Phys. Rev. Lett.*, 114:090502, 2015.
- [40] Mária Kieferová, Artur Scherer, and Dominic W. Berry. Simulating the dynamics of time-dependent hamiltonians with a truncated dyson series. *Physical Review A*, 99(4), Apr 2019.
- [41] D. W. Berry, A. M. Childs, Y. Su, X. Wang, and N. Wiebe. Time-dependent Hamiltonian simulation with  $l^1$ -norm scaling. *Quantum*, 4:254, 2020.
- [42] David Poulin, Angie Qarry, Rolando Somma, and Frank Verstraete. Quantum simulation of time-dependent Hamiltonians and the convenient illusion of Hilbert space. *Phys. Rev. Lett.*, 106(17):170501, 2011.
- [43] Dong An, Di Fang, and Lin Lin. Time-dependent hamiltonian simulation of highly oscillatory dynamics and superconvergence for schrödinger equation. *Quantum*, 6:690, 2022.
- [44] Kunal Sharma and Minh C. Tran. Hamiltonian simulation in the interaction picture using the magnus expansion, 2024.
- [45] Jan Lukas Bosse, Andrew M. Childs, Charles Derby, Filippo Maria Gambetta, Ashley Montanaro, and Raul A. Santos. Efficient and practical hamiltonian simulation from time-dependent product formulas, 2024.
- [46] Pablo Antonio Moreno Casares, Modjtaba Shokrian Zini, and Juan Miguel Arrazola. Quantum simulation of time-dependent hamiltonians via commutator-free quasi-magnus operators, 2024.
- [47] S Blanes, F Casas, J A Oteo, and J Ros. Magnus and fer expansions for matrix differential equations: the convergence problem. *Journal of Physics A: Mathematical and General*, 31(1):259, jan 1998.

- [48] A. Iserles and S. P. Nørsett. On the solution of linear differential equations in lie groups. *Phil. Trans. R. Soc. A.*, 357:983–1019, 1999.
- [49] S Blanes, F Casas, and J Ros. Improved high order integrators based on the magnus expansion. *BIT Numerical Mathematics*, 40(3):434–450, 2000.
- [50] A. Iserles, S.P. Nørsett, and A.F. Rasmussen. Time symmetry and high-order magnus methods. *Applied Numerical Mathematics*, 39(3):379–401, 2001. Themes in Geometric Integration.
- [51] Marlis Hochbruck and Christian Lubich. On Magnus integrators for time-dependent Schrödinger equations. *SIAM J. Numer. Anal.*, 41(3):945–963, 2003.
- [52] A. Iserles. *A first course in the numerical analysis of differential equations*. Number 44. Cambridge Univ. Pr., 2009.
- [53] S. Blanes, F. Casas, J. A. Oteo, and J. Ros. The Magnus expansion and some of its applications. *Phys. Rep.*, 470(5-6):151–238, 2009.
- [54] S Blanes, F Casas, J A Oteo, and J Ros. A pedagogical approach to the Magnus expansion. *Eur. J. Phys.*, 31(4):907–918, 2010.
- [55] Arieh Iserles, Karolina Kropielnicka, and Pranav Singh. Commutator-free magnus-lanczos methods for the linear schrödinger equation, 2017.
- [56] Sergio Blanes, Fernando Casas, and Mechthild Thalhammer. High-order commutator-free quasi-magnus exponential integrators for non-autonomous linear evolution equations. *Computer Physics Communications*, 220:243–262, 2017.
- [57] Arieh Iserles, Karolina Kropielnicka, and Pranav Singh. Magnus–lanczos methods with simplified commutators for the schrödinger equation with a time-dependent potential. *SIAM Journal on Numerical Analysis*, 56(3):1547–1569, 2018.
- [58] Guannan Chen, Mohammadali Foroozandeh, Chris Budd, and Pranav Singh. Quantum simulation of highly-oscillatory many-body hamiltonians for near-term devices, 2023.
- [59] Yuan Su. Fast-Forwardable Quantum Evolution and Where to Find Them. *Quantum Views*, 5:62, November 2021.
- [60] Di Fang, Lin Lin, and Yu Tong. Time-marching based quantum solvers for time-dependent linear differential equations. *Quantum*, 7:955, March 2023.
- [61] Dominic W. Berry and Pedro C. S. Costa. Quantum algorithm for time-dependent differential equations using dyson series, 2022.
- [62] R. L. Burden, J. D. Faires, and A. C. Reynolds. *Numerical analysis*. Brooks Cole, 2000.
- [63] András Gilyén, Yuan Su, Guang Hao Low, and Nathan Wiebe. Quantum singular value transformation and beyond: exponential improvements for quantum matrix arithmetics. In *Proceedings of the 51st Annual ACM SIGACT Symposium on Theory of Computing*, pages 193–204, 2019.

- [64] Christoph Sünderhauf, Earl Campbell, and Joan Camps. Block-encoding structured matrices for data input in quantum computing. *Quantum*, 8:1226, 2024.
- [65] Daan Camps, Lin Lin, Roel Van Beeumen, and Chao Yang. Explicit quantum circuits for block encodings of certain sparse matrices. *SIAM Journal on Matrix Analysis and Applications*, 45(1):801–827, 2024.
- [66] Haoya Li, Hongkang Ni, and Lexing Ying. On efficient quantum block encoding of pseudo-differential operators. *Quantum*, 7:1031, 2023.
- [67] Ryan Babbush, Craig Gidney, Dominic W Berry, Nathan Wiebe, Jarrod McClean, Alexandru Paler, Austin Fowler, and Hartmut Neven. Encoding electronic spectra in quantum circuits with linear t complexity. *Physical Review X*, 8(4):041015, 2018.
- [68] Kianna Wan. Exponentially faster implementations of select (h) for fermionic hamiltonians. *Quantum*, 5:380, 2021.
- [69] Diyi Liu, Weijie Du, Lin Lin, James P Vary, and Chao Yang. An efficient quantum circuit for block encoding a pairing hamiltonian. *arXiv preprint arXiv:2402.11205*, 2024.
- [70] Weijie Du and James P Vary. Hamiltonian input model and spectroscopy on quantum computers. *arXiv preprint arXiv:2402.08969*, 2024.
- [71] Andrew M. Childs and Nathan Wiebe. Hamiltonian simulation using linear combinations of unitary operations. *Quantum Information and Computation*, 12, Nov 2012.
- [72] D. W. Berry, A. M. Childs, and R. Kothari. Hamiltonian simulation with nearly optimal dependence on all parameters. *Proceedings of the 56th IEEE Symposium on Foundations of Computer Science*, pages 792–809, 2015.
- [73] Yuval R Sanders, Guang Hao Low, Artur Scherer, and Dominic W Berry. Black-box quantum state preparation without arithmetic. *Physical review letters*, 122(2):020502, 2019.
- [74] David Oliveira and Rubens Ramos. Quantum bit string comparator: Circuits and applications. *Quantum Computers and Computing*, 7, 01 2007.
- [75] Khuram Shahzad and Omar Usman Khan. A generalized space-efficient algorithm for quantum bit string comparators. *arXiv preprint arXiv:2311.06573*, 2023.
- [76] Maciej Zworski. *Semiclassical Analysis*. American Mathematical Society, 2012.
- [77] André Martinez. *An introduction to semiclassical and microlocal analysis*, volume 994. Springer, 2002.